INFORMATION TO USERS

This manuscript has been reproduced from the microfilm master. UMI films the text directly from the original or copy submitted. Thus, some thesis and dissertation copies are in typewriter face, while others may be from any type of computer printer.

The quality of this reproduction is dependent upon the quality of the copy submitted. Broken or indistinct print, colored or poor quality illustrations and photographs, print bleedthrough, substandard margins, and improper alignment can adversely affect reproduction.

In the unlikely event that the author did not send UMI a complete manuscript and there are missing pages, these will be noted. Also, if unauthorized copyright material had to be removed, a note will indicate the deletion.

Oversize materials (e.g., maps, drawings, charts) are reproduced by sectioning the original, beginning at the upper left-hand corner and continuing from left to right in equal sections with small overlaps.

Photographs included in the original manuscript have been reproduced xerographically in this copy. Higher quality 6" x 9" black and white photographic prints are available for any photographs or illustrations appearing in this copy for an additional charge. Contact UMI directly to order.

ProQuest Information and Learning
300 North Zeeb Road, Ann Arbor, MI 48106-1346 USA
800-521-0600

Université d'Ottawa • University of Ottawa

PREDICTING THE ICE CLEARING CAPACITY OF LAC ST-PIERRE

A thesis submitted in partial fulfillment of
the requirements for the degree of

Master's of Applied Science

Department of Civil Engineering
University of Ottawa

December 1999

Abstract

PREDICTING THE ICE CLEARING
CAPACITY OF LAC ST-PIERRE

Lac St-Pierre is particularly prone to ice jams that create difficult conditions for navigation on the shipping channel. In this project, a mathematical model was used to determine the ice clearing on Lac St-Pierre under various conditions. The particle-dynamics model Pdyn was applied to simulate a wide range of channel configurations and ambient environmental conditions. Relationships between ice movement and ambient conditions were then developed by aggregating the results from a large number of simulations.

The relationships obtained quantify the relative impact of various parameters, such as the channel geometry, floe size, ice concentration, and wind, on ice velocity and flux. And since it makes use of readily measurable field data, the mathematical model is particularly valuable for inclusion into an integrated ice management system.

Key-words: Ice clearing, transport, ice jam.

TABLE OF CONTENTS

page

LIST OF FIGURES

page

LIST OF TABLES

page

NOMENCLATURE

Symbol	Description
A_o	Area of open water
Ai	Ice surface area
b	Channel bottom width
B	Channel surface width
C_o	Initial ice concentration
C_{ice} or C	Ice concentration
C_A	Drag coefficient at the air-ice interface
C_w	Drag coefficient at the ice-water interface
D	Diameter of the ice floe
D_f	Accumulated freezing degree-day
F_{ice}	Ice flux
F_n	Normalised ice flux ($F_n = V_{ice}/(U\,B)$)
F	Froude number ($F = V / [g\,y]^{0.5}$)
Fr_d	Densimetric Froude number ($F_d = V/[\{1-\rho_i/\rho_w\}g\eta]^{0.5}$)
g	Gravitational acceleration constant (9.81 m/s^2)
h_i	Ice thickness
h_{sun}	Number of hours of sunlight
H	Water level
M_i	Mass of ice per unit surface area
q	Channel unit discharge ($q = Q_w/B$)
Q_i	Volume flow rate of ice
Q_w	Water discharge
Q_{dice}	Daily volume of ice formed
S_o	Channel hydraulic slope
T_a	Air temperature
T_m	Basal ice temperature
T_w	Water temperature
u or V_w	Current velocity
V_s	Surface water velocity
V_{ice}	Ice velocity
V_n	Normalised ice velocity ($V_n = V_{ice}/u$)
Vxi	Ice velocity in the x direction
Vyi	Ice velocity in the y direction
$Vwind$	Wind velocity
W	Scalar wind resistance ($W = V_{\text{wind}} \cos(\theta)$)
δ	Channel side slope
Y	Transverse distance measured from the centreline of the channel
κ	Coefficient of ice growth (Stephan formula)
λ	Latent heat of fusion for ice
ρw	Water density
ρ_A	Air density
ρ_i	Mass density of ice floe
θ	Angle between the wind direction and water current

Symbol	Description
σ_x	Ice stress per unit ice area normal to a channel cross section
τ_A	Wind shear stress, $\tau_A = \rho_A C_A V_A \lvert V_A \rvert \cos\theta$
τ_B	Bank resistance
τ_w	Water shear stress, $\tau_w = \rho C_w \lvert V_w - V_{ice} \rvert (V_w - V_{ice})$
ϕ_*	Net heat flux
ϕ_S	Net heat flux of short-wave radiation
ϕ_L	Net heat flux of long wave radiation
ϕ_H	Latent heat flux
ϕ_P	Precipitation heat flux
ϕ_P	Heat flux from flow friction
ϕ_G	Groundwater heat flux
ϕ_B	Bed heat flux
φ_c	Heat transfer coefficient
φ_a	Ice to air heat transfer coefficient
φ_w	Air to water heat transfer coefficient

ACKNOWLEDGMENTS

The present study was carried out at the Canadian Hydraulics Centre (CHC) of the National Research Council of Canada, with the financial support of the Canadian Coast Guard (CCG), Laurentian Region. My fellow colleagues at CHC and CCG personnel provided much appreciated and insightful comments throughout the project. I would particularly like to thank Dr. Mohamed Sayed of CHC and Dr. Brian Morse of CCG. I am grateful to Dr. Ron Townsend, my thesis director at the University of Ottawa for his patience and for his thoroughness in reviewing my work.

Finally, I also owe a great deal of appreciation to my loving husband, without the support of whom I may not have had the courage to finalise this document.

1 - BACKGROUND

1.1 Statement of the Problem

One of the most dramatic consequences of ice jams is the possibility of extensive flooding of the riverbanks, and therefore most of the research has focused on predicting the outset of these floods. Little is available on other aspects of ice management, particularly where winter shipping activities are concerned. Bank flooding and impediment on winter navigation are two problems that are fundamentally distinct. Floods typically occur during the break-up period, i.e. in the spring, and in rural areas where control structures are limited. For their part, shipping activities are mostly affected by ice jams or ice runs stoppage occurring during the winter when a channel artificially kept open fills with ice fragments, creating hazardous conditions or altogether preventing the passage of vessels.

In this work, we refer to ice jams as the stoppage of an ice run, i.e. when the ice stops circulating on the channel. The threshold at which this is observed is clearly much lower than that at which flooding becomes a concern.

In order to insure the safe passage of ships during the winter months, the transportation authorities, in Canada this is the Canadian Coast Guard, must carry out activities such as keeping an eye on ice concentration and movement on the river, dispatching icebreakers to maintain a certain channel width, and establishing speed limits to ensure proper development of an ice cover. One

problem that the authorities are facing is determining what conditions are likely to lead to an ice jam. The problem can be seen as a channel of finite dimensions, through which must pass a variable amount of ice arriving from upstream. The capacity of the channel to evacuate the ice as it arrives depends on various factors including the width of the channel, the quantity of ice to evacuate, and the resistance due to wind. When the ice supply from upstream exceeds the quantity of ice that can be evacuated by the channel, congestion can occur and, if this condition persists for a certain period of time, the flow of ice can stop altogether and completely obstruct the passage.

Figure 1 presents a view of winter conditions on the St. Lawrence shipping channel at Lac St-Pierre.

Figure 1: View of the shipping channel with ice.

The question thus becomes: How much ice can be cleared by a channel segment and cross-section under given conditions?

1.2 Objective and Scope of the Work

The objective of the present work is to gain a better understanding of how environmental and physical factors affect the movement of ice in a given channel and to develop a mathematical model or series of relationships for the prediction of the channel's ice clearing capacity. The Canadian Coast Guard would eventually like to use this mathematical model as a tool for ice management on Lac St-Pierre, a location historically prone to ice stops.

Some ice transport models exist and have been used in the past to study ice dynamics. These models have provided a wealth of valuable information and insight into the problem and possible cause-and-effect relationships. These models are however generally expensive from a computations standpoint and require a certain amount of effort in setting up and analysing the results. A certain amount of more qualitative information is also available but is dispersed and difficult to use "*as-is*" for the co-ordination of winter operations.

The Canadian Coast Guard has expressed interest in a simple method to predict the initiation of ice jams on Lac St-Pierre and to consequently take appropriate measures to prevent the closing of the shipping channel. A simple model or relationship may help meeting this goal by providing valuable information that can be used for daily ice management and operations. As such, the mathematical model, or relationships, developed should have the following characteristics.

- Be simple and easy to use.
- Make use of the information and results obtained by previous studies.
- Make use of data that can be readily measured on the field.
- Have theoretical/empirical foundations.
- Provide information that is directly applicable for decision-making.
- Be compatible with the ice management support system presently being developed by the CCG.

The present work focuses on the prediction of the clearing capacity of the channel at Lac St-Pierre. Ice production, although important and an essential component of river ice processes, is not covered in detail as an ice production model is being developed independently within the Canadian Coast Guard's organisation. The ice clearing mathematical model will eventually be part of a decision-support system that will be used for daily operational management. Therefore, it was important to keep in mind that inputs for the ice clearing component could eventually come from other components of the system, or from field monitoring data. A preliminary framework of the proposed ice clearing component of that system is schematised in Figure 2.

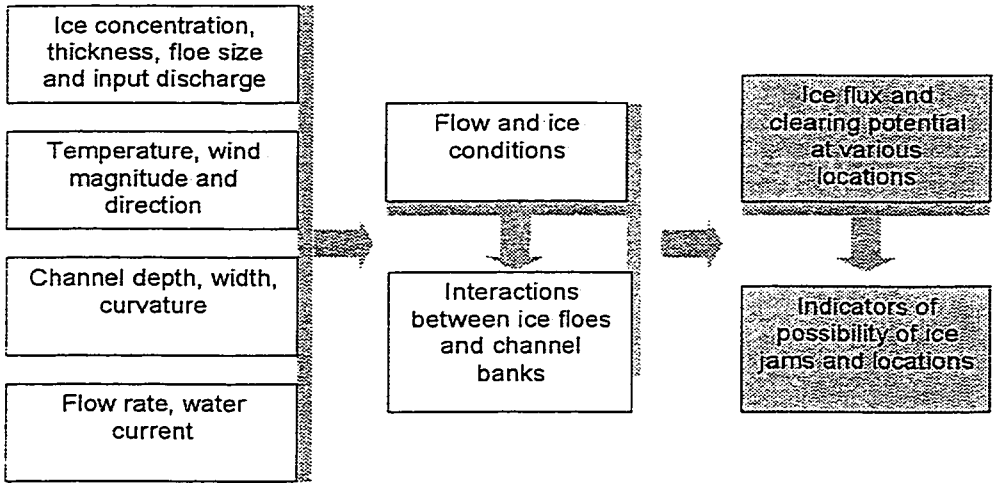

Figure 2: Ice Clearing Component

The most complex, and essential, part of the work resides in defining the relationships between the various components of the prediction model, i.e. the

relationships between the channel geometry, flow conditions, meteorology and resulting ice flux.

1.3 Uniqueness of the Contribution

There exist a certain number of numerical models that are currently being used to simulate river ice. Some of these models are very advanced and provide an accurate picture of the ice formation, transport and sometimes even the occurrence of ice jams and resulting flooding. However, these models are used for the most part in research or case-by-case studies of specific problems. They are typically computationally expensive and take a relatively long time to set-up, run and process the results. For example, a short simulation of CHC's Pdyn, a Lagrangian particle-dynamics ice model, takes approximately 3 hours to run on a fast PC, with only a limited number of particles (Sayed *et al.*, 1994). This is after extensive effort spent setting up the model. This is obviously not practical for day-to-day management operations where results must be produced regularly and in a timely fashion. Moreover, the ice observer or the operation manager may want to run various scenarios, or "what-if" cases, in order to get a better understanding of the influence of various factors before deciding on actions.

So, although ice dynamics theory and numerical models are available, they are often not in a form that can be directly used to provide quick predictions. The objective of this work was therefore to extract and aggregate as much

information as possible from the tools that are available and to develop a simpler, easier to use method.

1.4 Methodology

The work was divided into five main tasks:

1. Theoretical background and literature review on river ice processes and ice clearing predictions;
2. Review of historical data and results of previous studies on Lac St-Pierre;
3. Series of computer model simulations to quantify the impact of various factors on ice clearing;
4. Aggregation of simulations results to define relationships between channel characteristics, ambient conditions, and ice transport; and
5. Framework for including the ice clearing component and relationships developed into an integrated ice management tool.

A brief literature review is presented in Section 2 of the present document. Historical data and findings of previous studies on the movement of ice on Lac St-Pierre were also reviewed and are presented in sections 3 to 5.

1.5 Approach

The objective of this work was to integrate as much information, both theoretical and empirical, into a simple model or relationship relating environmental and

physical conditions to a channel's ice clearing capacity. The background information and data used in the development of the ice clearing mathematical model was obtained from four main sources:

- Theoretical/empirical equations from literature;
- Results from previous modelling studies of Lac St-Pierre by CHC;
- Field data obtained from CCG; and
- Additional computer simulations of the Pdyn model.

The field data and results from previous modelling studies were used to determine the range of conditions and existing data and identify possible gaps in the data. A range of conditions were identified and additional model simulations were carried out to provide corresponding ice clearing capacity. The simulations results provided the basis for the development of relationships between ambient conditions and ice clearing. The ice clearing relationships were then compared to equations found in literature and to results of another ice transport model.

2 - THEORETICAL REVIEW

A brief theoretical review of river ice processes is useful for a better understanding of the factors that affect ice jam initiation and to identify possible relationships between these factors.

2.1 Ice Formation and Growth

Even though the main interest of the present work resides in processes by which ice is being transported on a river, it is important to understand the factors that affect ice formation and growth, and hence the quantity of ice that will have to be cleared. Belthaos (1995) includes a general overview of the ice formation and growth processes that will be summarised in the following sections.

2.1.1 Heat Exchange in Open Channels

In laminar flow conditions, such as in lakes, the water is being cooled down at the interface with air and, as it becomes colder, sinks to the bottom of the water column to be replaced by warmer water (see Figure 3). This process continues until homogeneous conditions are attained at 4°C, the temperature at which the water density is at its maximum. Then, without further mixing, the surface water cools to the freezing point and an ice cover starts to develop. Once the water temperature reaches 0°C, any additional cooling results in ice formation.

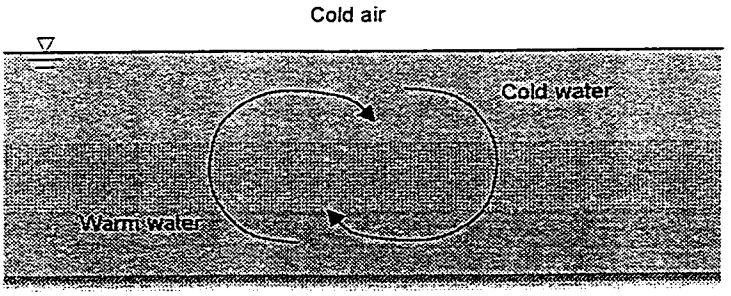

Figure 3: Heat exchange and mixing in laminar flow conditions.

In the case of turbulent flow, the existing vertical mixing suppresses the density stratification. The degree of mixing in the water column is expressed in terms of the density Froude number Fr_d.

(1.) $$Fr_d = \frac{U}{\sqrt{gH\Delta\rho_w / \rho_w}}$$

where U is the flow velocity (m/s), g is the gravitational acceleration (9.81 m/s^2), H is the depth of flow (m), $\Delta\rho_w$ is the density difference between the upper and lower layers (kg/m^3), and ρ_w is the density of the bottom layer water (kg/m^3).

At large values of Fr_d typical of rivers, the entire water column cools at the same rate and the water temperature change can be calculated based on the net heat exchange at the water surface.

(2.) $$\phi_* = \phi_S + \phi_L + \phi_H + \phi_E + \phi_P + \phi_F + \phi_G + \phi_B$$

where ϕ_* is the net heat flux, ϕ_E the net flux of short-wave radiation, ϕ_L the net flux of long wave radiation, ϕ_E the latent heat flux, ϕ_P the precipitation heat flux,

ϕ_F the heat flux from flow friction, ϕ_G the groundwater heat flux, and ϕ_B the bed heat flux (all in W/m^2).

In open-water conditions, the three last parameters of Equation 2 are small compared with the other parameters and can be neglected. However, in the case of ice-covered waters, they become non-negligible. The value of ϕ_S depends on atmospheric conditions such as the cloud coverage. It also depends on solar altitude and, as such, decreases at varying rates with the onset of winter. Values of ϕ_L, ϕ_H and ϕ_E are affected by the temperature difference between air and water. Wind speed also affects the value of ϕ_E.

Because of the difficulties in conducting energy balance studies, a more common semi-empirical approach is often used. In this approach, the net heat loss/gain is obtained by multiplying the water-to-air temperature difference by a heat transfer coefficient.

(3.) $\phi_* = \varphi_0 (T_w - T_a)$

where φ_0 is a heat transfer coefficient ($W/m^2°C$), T_w is the water temperature (°C), and T_a is the air temperature (°C).

Typical values of the heat transfer coefficient φ_0 range between 15 to 25 W/m^2 °C. Marcotte (1975) found φ_0 to be on average about 28 W/m^2 °C in

Montreal, but to rise to 59 W/m^2 °C under extremely cold and windy conditions (Beltaos, 1995).

2.1.2 Ice Formation

Ice formation takes place in successive stages that are characterised by the ice types present. The various types are defined by Beltaos (1995) as:

- Border ice: Border ice is the first ice that forms on bodies of water. It forms along the riverbanks or around obstacles to flow such as bridge piers. The existing border ice may become fragmented and detach from the shore following a change of water level or under the action of wind or ship waves.
- Moving level ice (also called "skim ice"): Often produced by thermal growth, skim ice comes in the form of large sheets of ice that are not attached to the shore.
- Frazil ice: Small ice particles that start to appear in the water column when the water reaches a small degree of super cooling, i.e. when the water temperature drops under the freezing point.
- Ice floes: Accumulation of frazil ice particles into larger floes sometimes used to describe moving level ice.
- Anchor ice: Ice that grows on the riverbed in very turbulent reaches.

2.1.3 Ice Production and Growth

It is possible to calculate the volumetric amount of ice being produced by an open-water reach in a given period of time by integrating the surface heat loss over time.

$$(4.) \qquad \forall_f = \frac{1}{\rho_i \lambda} \int_{t_1}^{t_2} A_0 C_0 (T_w - T_a) dt$$

where λ is the latent heat of fusion for ice (J/kg), ρ is the ice density, t_1 and t_2 are the initial and final time steps, respectively, A_0 is the area of open-water (m^2), C_0 is the initial ice concentration, and (T_w-T_a) is the difference between the water temperature T_w and the air temperature T_a (°C). This equation is of limited practical application however since, as border ice develops, the area of open-water A_0 is reduced by a fraction that is difficult to quantify.

Once the cover has formed, and as the freezing front migrates vertically downward into the water column, the ice thickness increases gradually. At the base of the ice sheet, the rate of ice growth is determined by the difference in ice heat fluxes at the ice under-surface and the water column.

$$(5.) \qquad \rho_i \lambda \frac{dh_i}{dt} = \frac{T_m - T_a}{\frac{h_i}{k_i} + \frac{1}{C_a}} - C_w (T_w - T_m)$$

where h_i is the ice thickness (m), k_i is ice the thermal conductivity (W/m°C), φ_a and φ_w are the heat transfer coefficients from ice to air and air to water, respectively (W/m^2°C), and T_m is the basal ice temperature (°C).

For many engineering applications, the subsurface heat flow is ignored and a more simplified approach is being used, such as the Stefan formula (Michel, 1971). The ice thickness is then a function of the accumulated degree-day:

(6.) $$h_i = \kappa\sqrt{D_f}$$

where h_i is the sheet ice thickness (m), D_f is the accumulated freezing degree-day, and κ is a coefficient that takes into account the conditions of exposure and surface insulation. Typical values for κ are presented in Table I. Note that Equation 6 gives inaccurate estimates of ice thickness for low values of h_i or D_f.

Table I: Coefficient for ice growth under varying conditions of exposure and surface insulation (Michel, 1971).

Conditions	κ (mm °C-1/2 d-1/2)
Theoretical maximum	34
Windy lake with no snow	27
Average lake with snow	17-24
Average river with snow	14-17
Sheltered small river with rapid flow	7-14

2.2 Ice Transport

Although ice formation and growth are obviously very important aspects of river ice processes, our main interest here resides more in the transport of this ice with the river flow. Ice transport is the subject of many papers and a number of approaches have been proposed to express the process mathematically. Three approaches will be presented in the following text: *(1)* continuum mechanics, *(2)* discrete particles, and *(3)* a mix of the two.

Figure 4 illustrates an idealised channel, while the forces that affect ice transport are schematised in Figure 5. Unless otherwise noted, the symbols used in all subsequent text are defined as presented on these figures.

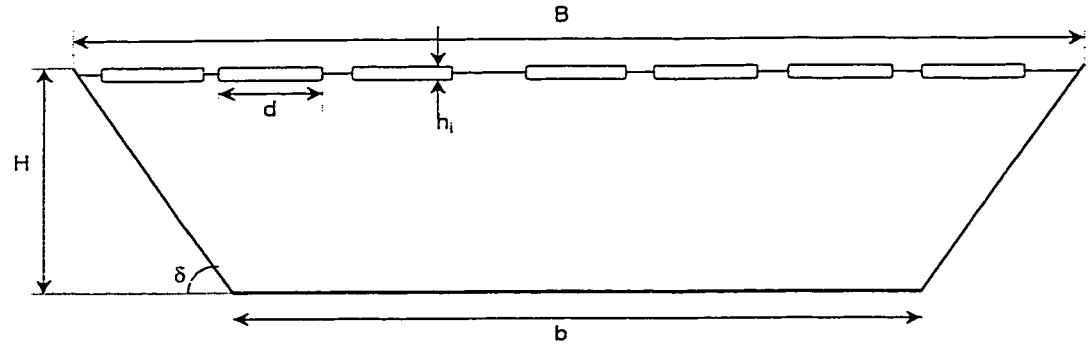

Figure 4: Cross-section of an idealised prismatic channel.

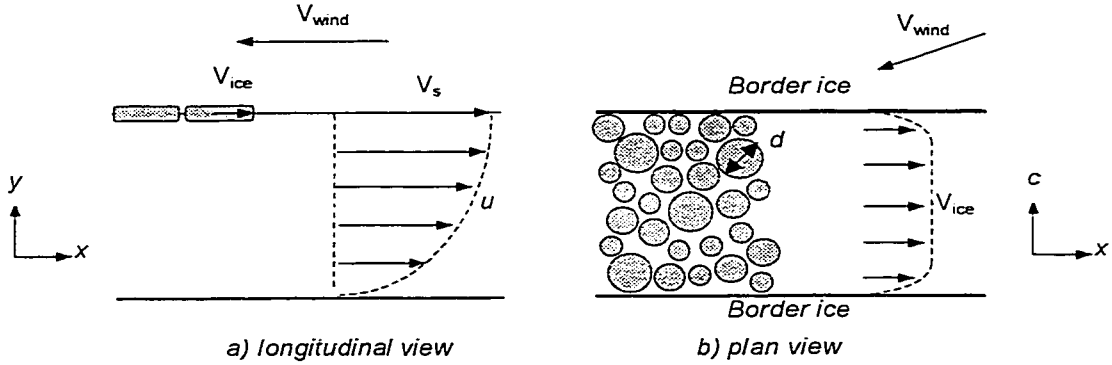

Figure 5: Forces affecting ice transport in a channel.

2.2.1 Continuum Mechanics Approach

Akerman and Shen (1983), Shen *et al.* (1991), and Shen and Lu (1996) present a theoretical formulation for the 2-D dynamic transport of river ice. The equation

of motion for the surface ice is obtained by considering the momentum balance of a differential area in the ice field:

$$(7.) \qquad M_i \frac{D\vec{V}_{ice}}{Dt} = \vec{R} + \vec{F}_a + \vec{F}_w + \vec{G} + \vec{V}_{ice}\vec{E}_m$$

in which

$$(8.) \qquad \frac{D}{Dt} \equiv \frac{\partial}{\partial t} + u\frac{\partial}{\partial x} v\frac{\partial}{\partial y}$$

where u and v are the x and y components of the ice velocity V_{ice}, M_i is the ice mass per unit area, R is the internal ice resistance force, F_a is the wind drag, F_w is the water drag, G is the gravitational force, and E_m is the rate of change of surface ice mass per unit area of water surface due to external sources and sinks.

The internal ice resistance R is calculated as:

$$(9.) \qquad \vec{R} = \vec{i}\left\{\frac{\partial}{\partial x}(\sigma_{xx}Ch_i) + \frac{\partial}{\partial y}(\sigma_{xy}Ch_i)\right\} + \vec{j}\left\{\frac{\partial}{\partial y}(\sigma_{yy}Ch_i) + \frac{\partial}{\partial x}(\sigma_{yx}Ch_i)\right\}$$

in which σ_{xx} and σ_{yy} are the normal stress components and σ_{xy} and σ_{yx} are the shear stress components.

In addition to the momentum equation, the conservation of ice mass equation can be written as:

$$(10.) \qquad \frac{D}{Dt}(\rho_i Ch_i) + \rho_i Ch_i \nabla \cdot \vec{U} = E_m$$

and the conservation of the ice area is written as:

(11.) $$\frac{DC}{Dt} + C\nabla \cdot \bar{U} = E_a - R_a$$

where ρ_i, C and h_i are the density, aerial concentration and thickness of the ice, respectively, E_a is the rate of change of the ice area concentration due to exchange between the surface and suspended ice and melting/freezing, and R_a is the rate of change due to mechanical redistribution.

Equations 7 to 11 can be used to solve for u, C and h_i, provided that relationships for the normal and shear stresses and the water flow condition can be established.

As the equations above indicate, the internal ice resistance affects the ice velocity in the channel. The ice velocity is also dependent on the water and wind drag and on the production rate. The internal resistance and bank shear is a function of ice concentration.

In 1-D and at low surface concentrations, the volume flow rate of ice can be expressed as:

(12.) $$Q_i = \int_0^B h \cdot C(y) \cdot u_i(y) dy$$

For a given channel geometry and water discharge Q_w, the ice discharge Q_i can be expressed in terms of the concentration of ice in the surface layer, as illustrated in Figure 6 where I represents the channel's ice conveying capacity.

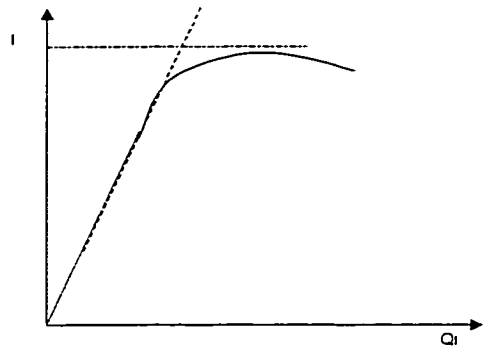

Figure 6: Relationship between ice discharge and concentration.

This relationship is nearly linear for low ice concentration. When the concentration of surface ice increases, the complete equation of motion has to be solved to accurately determine the relationship between Q_i and surface ice concentration.

A quantitative relationship was obtained by Ackerman et al. (1981) from a numerical solution of the equation of motion. A series of equations were developed for a range of geometries and flows representing physically realistic river conditions. Statistical analysis was performed on simulation results to obtain a more general equation that provides the ratio of the ice conveying capacity I to water discharge Q_w.

$$(13.)\ \frac{I}{Q_w} = 2.4\left(\frac{1}{\delta}\right)^{0.682}\left(\frac{h}{d}\right)^{1.181}\left(\frac{d}{B}\right)^{0.845\left(h/d\right)^{0.083}\left(1/\delta\right)^{0.106}}\left(\frac{gB^5S_0}{Q_w^2}\right)^{0.317\delta^{0.135}}$$

where S_0 is the hydraulic slope of the channel.

Equation 12 is valid for the ranges of values presented in Table II.

Table II: Range of validity for Equation 12.

Dimensionless variable	Range
d/B	0.001 to 0.1
d/h	Less than 1.0
Q^2/gB^5S_0	0.00002 to 0.2
δ	1:4 to 1:1/2

For a side slope of δ = 1:½ for example, Equation 12 can be approximated as:

$$(14.) \quad \frac{I}{B} = K\frac{h^{1.16}}{d^{0.33}}B^{0.13}S_o^{0.32}q^{0.36}$$

where I/B represents the maximum ice discharge by unit channel bottom width, q is Q_w/B, and K is a constant. We note from this equation that, as the characteristic dimension of the ice d increases, the ice-conveying capacity of the river decreases. Meanwhile, the ice-conveying capacity increases with increasing slope S_o and unit discharge q.

Although Equation 13 is relatively simple to apply, some of the parameters it requires, such as the channel slope, are more difficult to evaluate, let alone measure on the field. Moreover, the Equation assumes a simplified channel with a trapezoidal cross-section and neglects important factors, such as the effect of wind magnitude and direction on ice transport, the presence of border ice, and thickening of the ice by floe accumulation.

In Ackerman's equation, the ice is represented as a single body, i.e. no distinction is made between ice floating at the surface and ice transported in the water column. Shen, Wang and Lal (1995) developed a two-layer ice-transport concept that was introduced in their mathematical model, on which the RICE numerical model is based. The model is schematised in Figure 7.

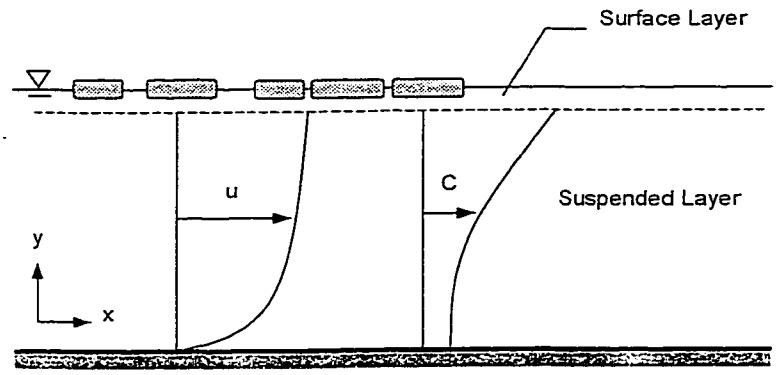

Figure 7: Definition of the RICE mathematical model.

In this 1-D model, the total ice discharge is first calculated for a given reach. The ice discharge is then separated into suspended-ice and surface-ice discharges based on distribution coefficients. Ice discharges are expressed, respectively, as:

(15.) $Q_d^i = AuC_f$

(16.) $Q_s^i = BuC_{ice}\left[h_i + (1-e_f)h_f\right]$

where Q_d and Q_s respectively represent the volumetric rate of ice discharges in surface and suspended layers, h_i is the solid ice thickness, h_f is the thickness of the frazil ice layer and e_f its porosity, C_{ice} is the area concentration or the fraction of water covered by ice, C_f is the volumetric concentration of frazil ice in the

suspended layer, A is the flow area, B is the channel width, and u is the mean flow velocity.

2.2.2 Discrete-Particles Approach

A second approach has been used in modelling ice transport whereby, instead of the continuum mechanics approach presented in the previous section, a Lagrangian particle approach is followed. In this second approach, the ice is modelled as discrete elements, or particles, that are being displaced under the resulting action of water current, wind shear, interactions between the particles, etc. The position of each particle is tracked at each time step of the simulation, therefore providing an accurate image of forces and ice movement. The applicability of such an approach relies on efficient tracking of the large amount of information generated during a simulation. The Lagrangian discrete particle approach has been used by Shen *et al.* (1993) and Sayed *et al.* (1994) for modelling ice dynamics. It has the advantages of providing a very accurate representation, ice floe by ice floe, of the interactions occurring within the ice field.

The Pdyn model (Sayed *et al.*, 1994, and Serrer *et al.*, 1997) is an application of the discrete-particle approach. In this model, schematised in Figure 8, the ice floes are modelled as rough inelastic disks. These disks can be joined at random in groups of two, three and four disks, resulting in irregular shapes that account for the interlocking that may occur between ice floes.

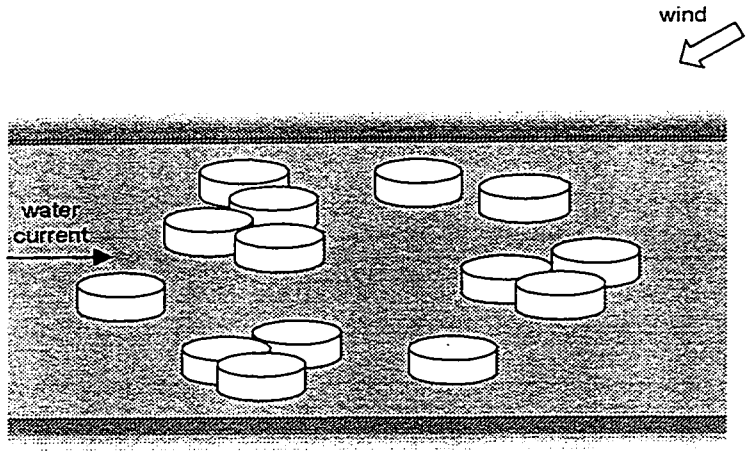

Figure 8: CHC Pdyn discrete-particle model.

The Pdyn model keeps track of the instantaneous position and velocity of each individual particle forming the ice field. At each time step and for each particle, the overlap between neighbouring floes and resulting contact forces are calculated. Wind and water drag forces are then added and accelerations determined from the resultant force. The velocity is obtained by integrating the accelerations. This procedure is repeated at each time step for the duration of the simulation.

The balance of linear momentum for each floe is expressed as:

$$(17.) \qquad m\frac{d\bar{u}}{dt} = A\tau_a + A\tau_w + \sum_{i=1}^{n}\bar{F}_n$$

where m is the mass of the ice floe, u and A its velocity, and area, respectively, and $\sum_{i=1}^{n} F_n$ is the sum of contact forces due to n contacts with other ice floes.

The wind and water shear stresses are calculated using, respectively:

(18.) $\tau_a = C_a V_a^{\,2}$

(19.) $\tau_w = C_w (V_w - u)^2$

where C_a and C_w are the coefficients of air drag and the water drag, respectively, and V_a, V_w and u are the mean velocity of the air, water and flow, respectively.

The balance of angular momentum of a floe is given by:

(20.) $$J\frac{d\omega}{dt} = \sum_{i=1}^{n} T_i$$

where J is the moment of inertia of the ice floe, ω its angular velocity, and $\sum_{i=1}^{n} T_i$ the sum of the torques due to n contacts with other ice floes.

The Pdyn model was applied to Lac St-Pierre during two studies, the first in 1994 (Sayed *et al.*, 1994) and the second in 1997 (Serrer *et al.*, 1997). The model was verified with existing data and was found to reliably predict ice transport in the shipping channel. Unfortunately, set-up and computations are very time intensive even using the latest microprocessors, which greatly limit the model's use for a quick and easy response, or as an operational prediction tool.

2.2.3 Mixed Approach

The most recent development in modelling ice transport consists in combining the high accuracy of the Lagrangian models with the efficiency of Eulerian-based calculations. This approach was selected for the recent development by Sayed

(1999) of the Ice Module of Environment Canada's Community Ice-Ocean Model (CIOM). Still in its preliminary development phase, the model uses a particle-in-cell (PIC) method, whereby velocities of individual particles are determined by interpolating velocities at the nodes of an underlying eulerian grid of a larger scale. The individual particles are then advected and an average cell ice mass and thickness is calculated for each eulerian grid node. This method allows an accurate mapping of ice thickness and concentration throughout the ice field.

2.3 Ice Jams

2.3.1 Formation of ice jams

In rivers, the majority of the ice floes are transported on or near the water surface. If this flux is arrested for any reason, or if the ice transport capacity of the river is reduced locally, an ice jam may form. The exact conditions that lead to the formation of an ice jam are difficult to quantify, although various ways in which this jam may occur have been described.

When the incoming ice discharge (Q_i) exceeds the local ice transport capacity of the stream (I), congestion occurs. Congestion due to a natural constriction or as a result of the presence of border ice is illustrated in Figure 9.

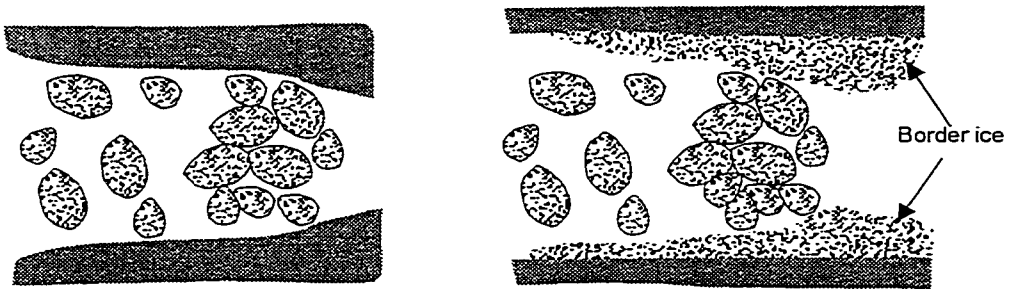

Figure 9: Congestion at a natural constriction and due to the presence of border ice.

In the case where the current velocity is slow enough so that the floes are not submerged, a surface jam is initiated. The mechanisms by which a single-layer ice jam is formed are schematised in Figure 10. The sequence of the figures follows an increasing B/d ratio.

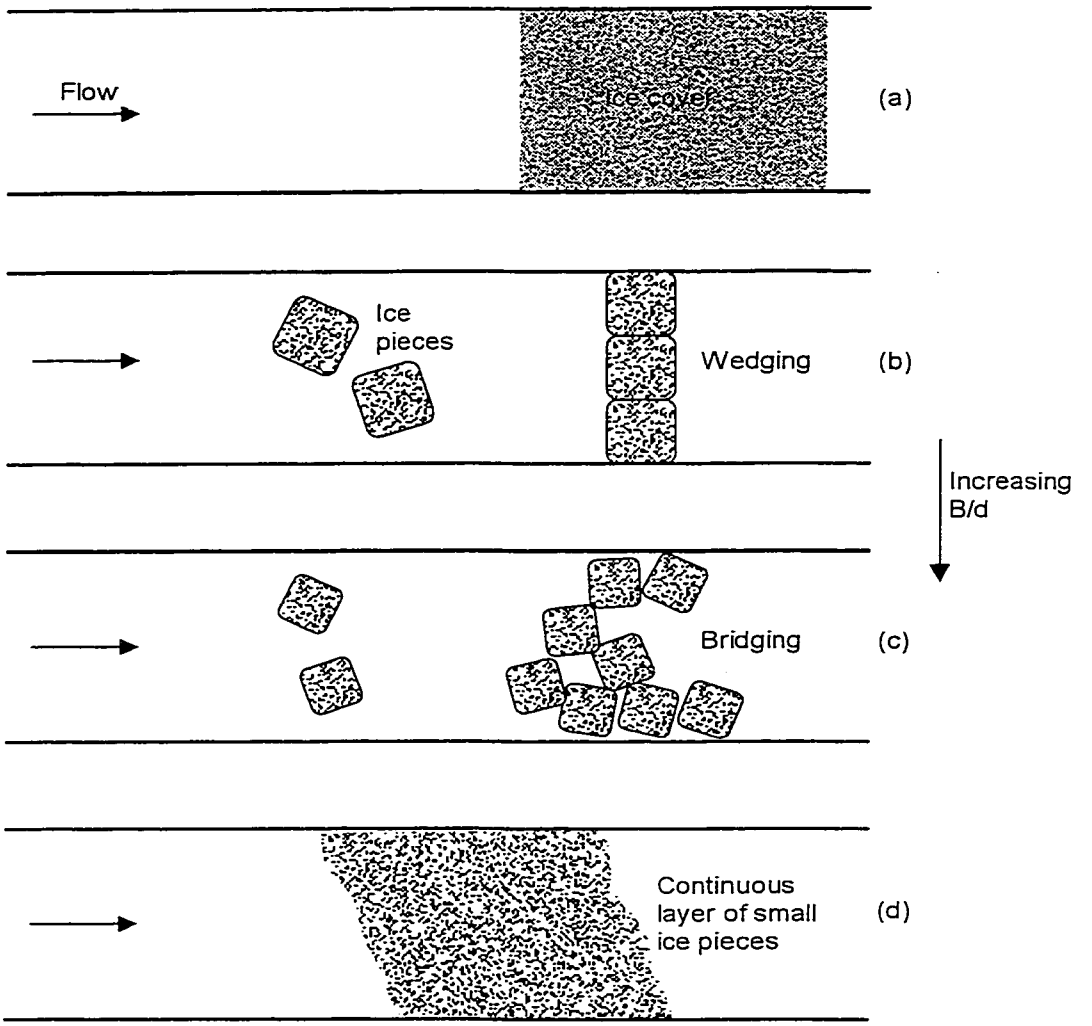

Figure 10: Mechanisms of surface ice jam initiation.

The simplest mechanism is a single obstruction (Figure 10 (a)), such as the presence of an ice cover spanning a channel at a downstream section. The next mechanism is wedging (Figure 10 (b)). It occurs when several pieces wedge between channel walls. Wedging is limited to relatively large ice pieces, when B/d is less than about 10. Increasingly complex assemblages of pieces are needed to

initiate a jam when the B/d increases beyond 10, because a lot more pieces are necessary to span the channel. Calkins and Ashton (1975) and Tatinclaux and Lee (1978) have shown that when B/d is less than about 15 to 20, jamming may be initiated by a single layer of ice floes lodged against one another to form an arch (Figure 10 (c)). The mechanism is diversely referred to as bridging, congestion jamming, lodgement, or arching. Ackerman and Shen (1983) and Shen *et al.* (1988) have examined maximum ice conveyance, when B/d is of the order of 1000 and less. Ackerman and Shen developed an expression used in determining the maximum discharge that is associated with conveyance of ice in a single layer (Figure 10 (d)). This expression was presented in Section 2.2.2.

2.3.2 Predicting the initiation of an ice jam

A limited number of studies have been published on the factors leading to the formation of an ice jam. In such a study, Ettema (1990) found that congestion can occur even under uniform flow conditions, i.e. without the presence of constrictions or speed reduction. It can, for example, be due to an increase in surface concentration of ice caused by higher bank resistance. It may also be promoted by strong adverse winds (blowing in the upstream direction) that create a significant resistance to the downstream movement and reduce the ice transport capacity of the river segment. This is more particularly prominent on large rivers or where the rivers flow into large expanses of water such as lakes and seas.

Ettema's study included a large series of laboratory experiments on the initiation of ice jams in channels of different configurations and under various flow conditions. He found that the initiation of an ice jam depended on the flow Froude number F ($F = u/(gy)^{0.5}$; where u is the flow velocity, g the gravitational acceleration, and y the water depth), as presented in Figure 11. He also found that the length of channel required for a jam to form and the jam thickness increased with increasing F.

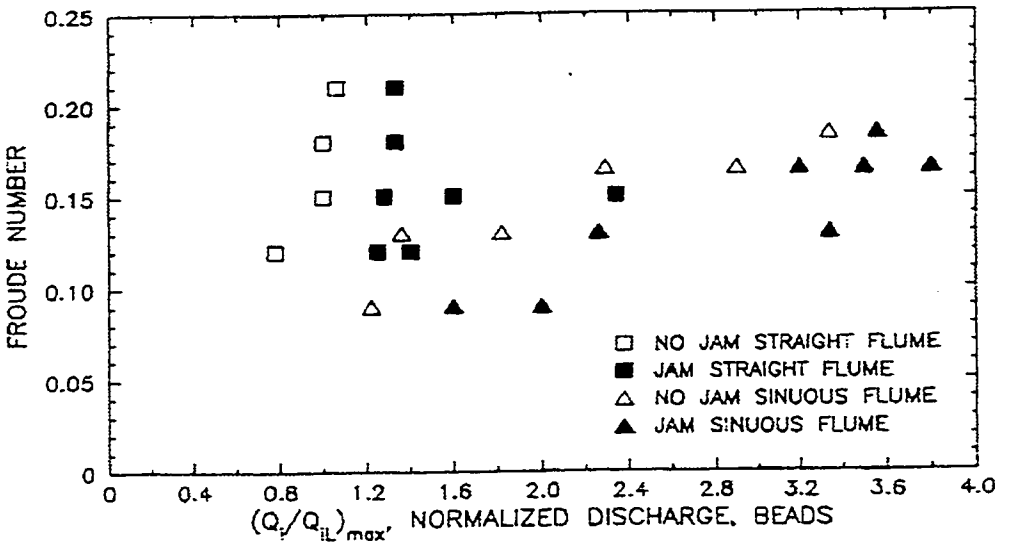

Figure 11: Initiation of ice jam in straight and sinuous flumes (from Ettema, 1990).

Similarly, Urroz and Ettema (1994) conducted small-scale experiments on ice-jam initiation in a curved channel. Their study showed that ice conveyance in a curved channel takes place non-uniformly and unsteadily, such that bunching occurs easily. Maximum ice conveyance was limited by two mechanisms: (i) lodgement

when the ice fragments are large relative to the channel width, and (ii) gorging when ice pieces are relatively small. They found that the initiation of ice jams by gorging depended on the Froude number as illustrated in Figure 12. In this figure, the normalised ice discharge represents the ratio of the volumetric ice discharge (Q_i) to the ice discharge corresponding to the maximum possible ice-floe surface concentration (Q_{iL}).

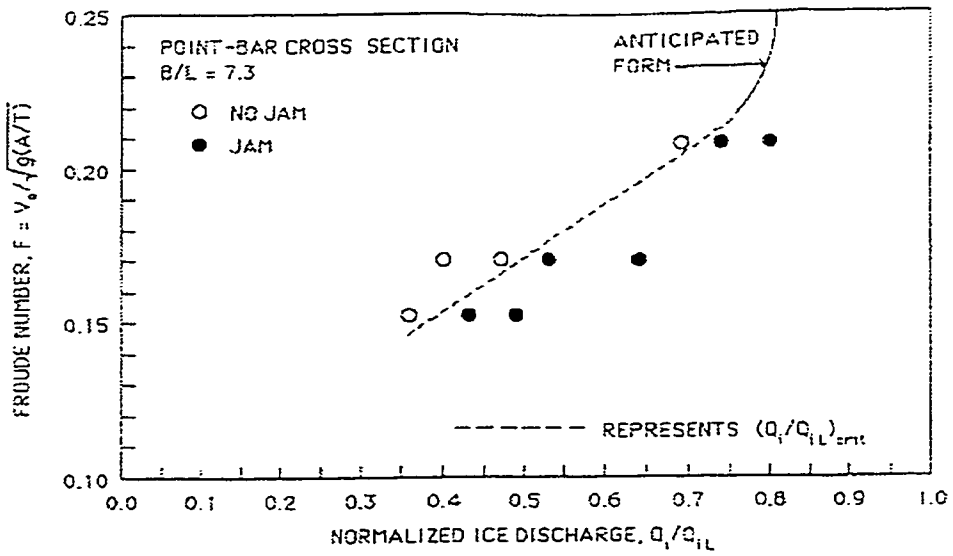

Figure 12: Relationship between the ice discharge and the Froude number and its impact on ice jam formation (Urroz and Ettema, 1994).

Laboratory studies, such as the ones reported in Ettema (1990) and Urroz and Ettema (1994) often assume that all of the ice flux occurs in a single surface layer and the cover initiating the jam is unbreakable. Such assumptions are realistic where freeze-up phenomena are concerned or in cold weather.

2.3.3 Identification of Ice Jamming Sites

Once the factors or conditions promoting the formation of ice jams are known, it may be possible to identify, for a given river, the reaches in which these conditions are more likely to occur. Probabilities of an ice jam are higher at sites exhibiting certain natural or man-made morphological features. These can for example be natural or artificial constrictions and sites presenting slower water currents. Such reductions in width or velocity entail increased concentrations of ice, eventually causing an ice jam. Constrictions may also contribute in ice jam initiation by preventing the free movement of large ice sheets, which may become lodged. As seen in the preceding section, the same can be attributed to river bends. Areas of low velocity or marked slope reduction are prime candidates for formation of an ice jam due to an increase in surface ice concentration and subsequent congestion. Wind is another important factor that affects ice transport.

Nuttall (1973) presents a simplistic approach to identify possible ice jamming sites. The criteria for initiation of an ice jam are a surface ice discharge coefficient and the Froude number. The ice discharge coefficient is defined as:

(21.) $$C_i = \frac{A_i}{C_S Q_w} y_m$$

where C_s has values ranging from 1.2 in a long, straight reach, to 1.0 in contractions (channel width reductions), and y_m represents the hydraulic mean depth (A/B).

The critical value of C_i for which an ice bridge may form has been found to be around 1.0. It is not however a sufficient criterion for formation of an ice jam. Nuttall also observed that the ice bridge will not form unless the local Froude number is less than about 0.08.

3 - ICE MANAGEMENT ON LAC ST-PIERRE

Although the St-Lawrence River is relatively well behaved, if left to its natural state, a series of ice jams would take place each winter. In the past, floods were a natural phenomenon that took place every year. The Canadian Coast Guard equipped itself with a crew of icebreakers following deaths caused by floods at the end of the 1800's. Initially, the icebreakers were used only to clear the ice on the river, before the spring melt. The crew was augmented in the 1960's to also provide protection against ice jams forming in the beginning of the winter.

In parallel, various ice control structures were constructed. A permanent ice regulator was built 100 m upstream from Champlain Bridge in order to minimise risks of flooding at Montreal. This is in addition to ice booms at Lavaltrie, Lanoraie and Yamachiche (Lac St-Pierre). Since then, one of the main goals of the Canadian Coast Guard has been to prevent formation of ice jams. Generally, this is achieved with success. There has not been any major flood caused by ice jam since the beginning of the program.

Commercial shipping is taking advantage of the fact that part of the St-Lawrence River stays open throughout the winter. The Canadian Coast Guard has added escort services to its ice management activities. As a result, ports located on the St-Lawrence can do business all throughout the year. In fact, the time between

last departures and first arrivals at the Port of Montreal has been shortened from about five months at the beginning of the century to year-round navigation today. Figure 13 shows the number of days that the channel was closed to navigation from 1961 to today. As we can note, Coast Guard's activities have generally been very successful in reducing down time. An interesting fact to note, the last three major closings (i.e. 84-85, 92-93 and 93-94) took place at the same location in Lac St-Pierre.

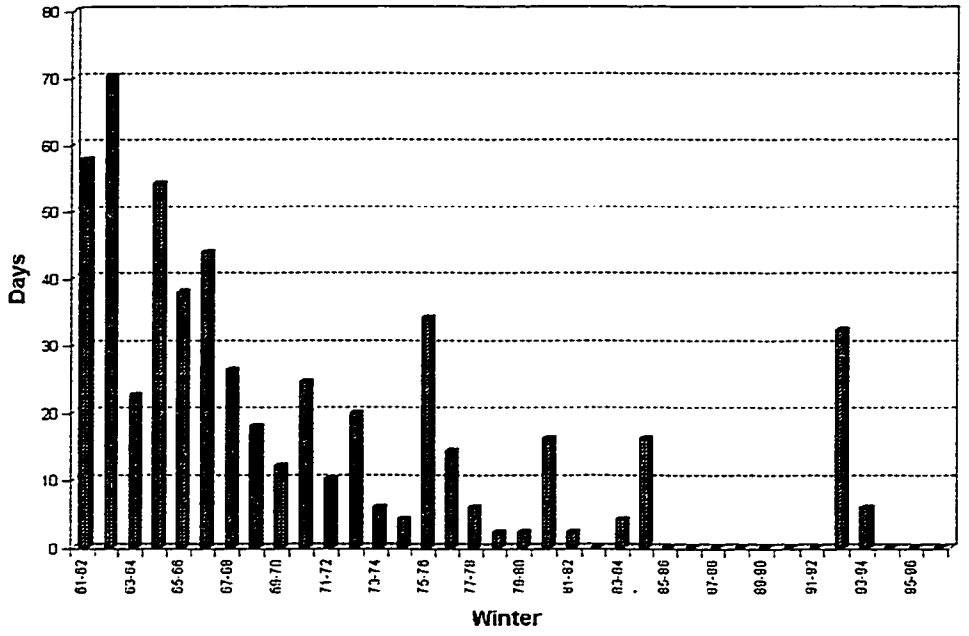

Figure 13: Number of days the shipping channel was closed due to ice between Quebec City and Montreal, 1961 to 1997 (from CCG information).

A crucial parameter in icebreaking operations is the width of the open channel. The lane must be wide enough to permit safe navigation and adequate ice evacuation. Yet, a wider channel may also mean increased operational difficulties and expenses.

3.1 Anatomy of Lac St-Pierre

To insure proper ice management on the river, the CCG must keep an eye on problematic sectors. The Ice Bureau pays special attention to Laviolette and Quebec bridges. By keeping an eye on ice conditions on the river, the Bureau can also identify locations where the ice cover may separate. However, the most problematic location remains a 30-km long widening of the river located midway between Montreal and Quebec that is known as "Lac St-Pierre" (Morse, 1994). The river is approximately 14 km wide at that location, i.e. 5 times larger than upstream. Also, due to a very small gradient of 15 to 30 cm between inlet and outlet, the currents are low. In Lac St-Pierre, further complications arise from pieces of the ice cover that may break off under the action of the wind and waves from passing ships. These large masses can move into the shipping lane and effectively block it. One of the most troublesome areas in this matter is the Northeast section of Lac St-Pierre (Lawrie, 1972).

A number of studies have concentrated on suggesting interventions to reduce the risks of ice jams on Lac St-Pierre. Essentially, the solution comprises two main aspects (Dumont, 1997):

1) Reduce the quantity of ice entering the channel;
2) Increase the ice clearing capacity of the shipping channel.

Examples of how these aspects can be realised through ice management activities include:

- Reducing the free water surface upstream from Lac St-Pierre by installing structures that promote the development of a stable cover;
- Promoting the formation of a stable ice cover outside the shipping channel;
- Limiting perturbations of the formed ice cover by keeping a tight control on icebreaking activities and limiting the speed of commercial vessels;
- Maintaining the channel width through icebreaking operations.

The following sections present findings of previous studies that focused specifically on Lac St-Pierre, identifying the major factors affecting ice processes and clearing capacity of the shipping channel.

3.1.1 Ice Production

Meteorological conditions such as temperature and sky cover directly influence the ice production upstream and on the lake. Wind affects the shear stress on ice cover and water areas, and can greatly modify surface velocities and the clearing capacity of the channel.

Once the water temperature of the river drops to the freezing point, any heat transfer is converted into ice production. The amount of ice formed is then proportional to the temperature and was estimated to be approximately equivalent to 6 mm of ice per degree C below the freezing point, per day (Morse, 1994). This ice is formed wherever the river is not already covered with ice, and the volume of ice produced is therefore a function of the fraction of ice cover. A portion of the ice produced upstream from the lake goes into the development of the cover. Once the cover is complete up to Montreal, except for the navigation channel, extra ice production has to be flushed through the channel.

A model was developed by the Canadian Coast Guard (CCG) to determine the daily volume of ice that enters Lac St-Pierre (Siles, 1997). The model is based on an equation selected by the Joint Board of Engineers in 1926. This equation was inspired from Equation 3 of the present document and is expressed as:

$$(22.) \quad Q_{d\,ice} = \frac{95(T_w - T_a)A}{144 \times 57.4 \times 27}$$

The daily volume of ice formed, Qd_{ice}, is expressed in cubic yards, the air temperature T_a represents the median temperature from minima and maxima and the area of open water A is expressed in cubic feet. Equation 22 was validated in three studies (Siles, 1997), the first two by Hydro-Quebec in 1947-48 and 1949-50 (Hydro-Quebec), and a third study in by the Canadian Coast Guard in 1997.

The CCG model makes some corrections to the predicted ice formation to account for sky coverage and wind. The corrections are calculated from relationships developed in a previous study by Laboratoire Lasalle (1959).

(23.) $$Q_{d\,sun} = 0.00037688 \times 10^{-4} (h_{sun} - 5) \times 3600 \times 24 \times A$$

where h_{sun} is the number of hours of sunlight.

(24.) $$C_{wind} = \frac{(-0.0042T_a + 0.75)\left(\frac{Q_{d_{ice}}}{1.609}\right) + (-0.05T_a - 0.2)}{12(-0.0042T_a + 0.75) + (-0.05 - 0.2)}$$

The volume of ice produced Qd_{ice} obtained in equation 22 is thus adjusted with a volume Qd_{sun} and then multiplied by the wind correction factor C_{wind}.

By studying aerial photographs gathered over a period of ten years, Siles (1997) identified 41 characteristic areas between Trois-Rivieres and Lac St-Louis. The Canadian Coast Guard ice production model calculates, for each of the characteristic areas, the ice volume produced based on temperature, sky cover and wind conditions. The ice is then routed downstream. As a result, the ice entering Lac St-Pierre at any moment in time is composed of ice from various location and production dates.

3.1.2 Wind

Wind plays a role in ice production by increasing the thermal exchange between water and air. Morse (1994) for example, reports that there is approximately 70%

more ice being produced under a wind of 20 knots (10 m/s) than at 10 knots (5 m/s).

Also, the wind plays a crucial role in ice clearing capacity. The wind shear stress on the ice and water surfaces can greatly modify the surface water velocity and, consequently, the ice drifting velocity. Observers note that, on Lac St-Pierre, the ice can stop when a wind from the NE is higher than 10 to 15 knots (Morse, 1994). This is in agreement with numerical simulations of Curve 2 by Sayed *et al.* (1994), which have shown that a wind of 15 knots from the NE resists the ice flow, decreasing the flux by about 25%.

3.1.3 Channel Geometry

As seen in Section 2.3, the channel geometry, particularly the width and curvature, are major factors in the initiation of an ice jam by promoting congestion and subsequent jamming.

Sayed *et al.* (1994) carried out numerical modelling of the influence of the channel geometry on the ice flux passing through Curve 2. The model has shown an increase in the ice flux of the order of 20% after smoothing the curvature at that location, while the ice velocity was essentially unchanged. Various channel widths were investigated. A width increase of 30 m (or 12.5%) from the initial width of 274 m resulted in an increase of ice flux of about 20%. Decreasing the width by the same amount decreased the flux by 34%.

3.1.4 Hydraulics

Water levels on Lac St-Pierre depend on various factors: flow, wind, tides, vegetation, ice cover, etc. Although not considered in the "tidal zone" of the St. Lawrence River, Lac St-Pierre shows tidal level variations of about 10 cm. The effect of tides on currents can be noted up to Curve #1. In the Yamachiche sector for example, the difference in currents amplitude between high and low tide cycles is approximately 5 cm/s, or 25%.

The presence of an ice cover along the banks of the lake contributes to increasing water discharge in the shipping channel. For example, an ice cover of 60 cm can reduce the hydraulic section by about half, increasing the water flow in the channel by as much as 60% (Morse, 1994).

3.1.5 Additional Factors

In addition to morphological and climatic factors, shipping activity, particularly the speed of passing vessels, influences the stability of the lake's ice cover. Waves produced by vessels moving at high speed may fracture the ice cover. The fragments can separate from the border ice and be carried into the shipping channel. Studies carried out in 1967-69 showed that critical factors are the type of vessel, the depth of the channel and surrounding areas, and the ice thickness and strength.

In order to protect the recently formed ice cover, the Canadian Coast Guard has imposed, since 1969, strict restrictions on vessel speeds. At the present time, the allowed speed is 10 knots, measured relative to current velocity.

4 - REVIEW OF HISTORICAL INFORMATION AND AVAILABLE DATA

Dumont (1997) attributes the initiation of most ice jams upstream from Montreal to lower ice clearing rates due to lower current velocity or adverse winds. Two main ice jams events have been documented in reports obtained from the Canadian Coast Guard (CCG). These two events will be summarised in Section 4.1. Current CCG activities related to the management of ice in the shipping channel will be presented in Section 4.2

4.1 Reported Ice Jams

4.1.1 Ice Jams of 1985

In his report, Simard (1985) describes the conditions that led to the ice jam on Lac St-Pierre on January 16-25, 1985. The St-Lawrence Seaway Authorities had decided to delay the closing of the shipping channel until December, if possible. This was to allow enough time for all commercial vessels to return to the sea. In order to prevent the formation of an ice cover, the water current, and therefore the water discharge were maintained abnormally high. After the closing of the shipping channel, the flows would be lowered considerably in order to allow the ice cover to form.

The flow was therefore maintained between 7300 m^3/s and 8000 m^3/s until December 29th. In a last effort to keep the shipping channel open, the flow was even increased to 8600 m^3/s on December 30th. During the following six days, the flow was reduced gradually to reach 6400 m^3/s on January 5th. The flow was further reduced to its minimum value of 5900 m^3/s on January 17th. This diminution of flow resulted in a diminution of the current velocity of about 0.6 m/s (1.95 ft/s), assuming that 80% of the flow goes in the shipping channel. It is on that date that ice jams began to form, first at Batiscan, then upstream of Curve #2 on Lac St-Pierre. The ice jam cleared eight days later on January 25th following an increase in discharge to 6800 m^3/s (water current increase of about 0.30 m/s or 1 ft/s).

The ice jam is attributed to a combination of factors: increased ice production due to the large areas of open water, low current velocities resulting from the discharge reductions, and once the ice jam formed at Batiscan, the almost null current velocity in the shipping channel in Lac St-Pierre. The intervention of icebreakers was complicated by the fact that, the velocities being small, as soon as an ice jam was dislodged, another one would form downstream. During this event, the determining factor seems to have been the very low velocity in the channel.

4.1.2 Ice Jam of 1993

The 1992-93 winter was very mild. The St-Lawrence River was mostly open water between Montreal and Trois-Riviere. The north side of Lac St-Pierre was open, as well as the sections upstream from Lanoraie and Lavaltrie ice booms. The current in the shipping channel easily transported the ice produced on these open water areas. In fact, the Coast Guard was so optimistic that it had started to make preparations for the spring break-up.

However, the temperature dropped severely in the third week of January. This greatly increased the volume of ice produced. After a certain time, Lac St-Pierre was barely sufficient to carry the ice, let alone the additional ice being produced on the lake itself. At this point, any change in the weather conditions (drop of air temperature, stronger wind, wind from the direction opposite to the flow) would initiate an ice jam. The ice jam formed at Curve #2 first and then spread upstream to Curve #1. In addition to the problem of clearing the ice from upstream, the lake quickly covered with ice that increased in thickness with time and spread over the lake. The ice eventually covered Curve #3 and Nicolet, completely blocking the passage. The currents, small at the best of times, were now completely stopped. Some time after the formation of the ice jam, the surface water tried to pass the ice jam by passing either under or on either side. It eventually formed a secondary channel, reducing even more the flow in the shipping channel and worsening the situation.

Simard (1993) qualifies the ice jam of 1993 as representative of 99% of ice jams that occur on Lac St-Pierre. The determining factor here seems to have been the combination of a sudden increase in ice concentration and a decrease in channel width.

4.2 Data Collection Activities

During the last few years, instruments have been installed at various locations between Quebec City and Montreal to record ice movement and meteorological conditions along the shipping channel. The type of information collected is particularly relevant for the development of an ice clearing prediction tool to be integrated within an ice management system since it determines what the inputs to the model may be. Table III presents an inventory of the monitoring equipment currently in place.

4.2.1 Ice Information

The ice conditions are provided by ice charts in the standard format of the Ice Centre of Environment Canada. The charts are produced daily at the Quebec Office, following observation flights over the St-Lawrence River. Figure 14 shows the ice chart of Lac St-Pierre for the 22nd of January, 1996.

Table III: Ice management instrumentation, Laurentian Sector.

Location (following direction of the flow)	Type of instrument						
	Fixed camera	Directional camera	Time laps video	Radar	Load sensors	Inverse sonar	Weather station
Lavaltrie ice boom	■		■		■		
Lanoraie ice boom					■		
Tracy	■						
Ile des barques		■		■			
FA Curve #2 upstream			■				■
FA Curve #2 downstream	■						
FP Curve #2 downstream		■		■			
Island #3	■		■			■	
Yamachiche ice boom					■		
Island #4	■		■				
Laviolette bridge		■					
Pierre-Laporte bridge		■		■			

The ice characteristics are indicated using the standard Environment Canada egg-symbols shown at the bottom of Figure 14. The symbols comprise four different sections, as shown is Figure 15. From top to bottom, they are: the total ice coverage, the fractions of each ice type, the types of ice present, and the size of the ice floes.

The ice charts provide some good information on the general ice conditions found on the St-Lawrence. However, they also have their limitations. The ice codes were mostly developed for the Arctic and a lot of the ice types and forms

are only found in the Arctic (multi-year ice for example). Also, the ice contours are drawn on the charts only approximately.

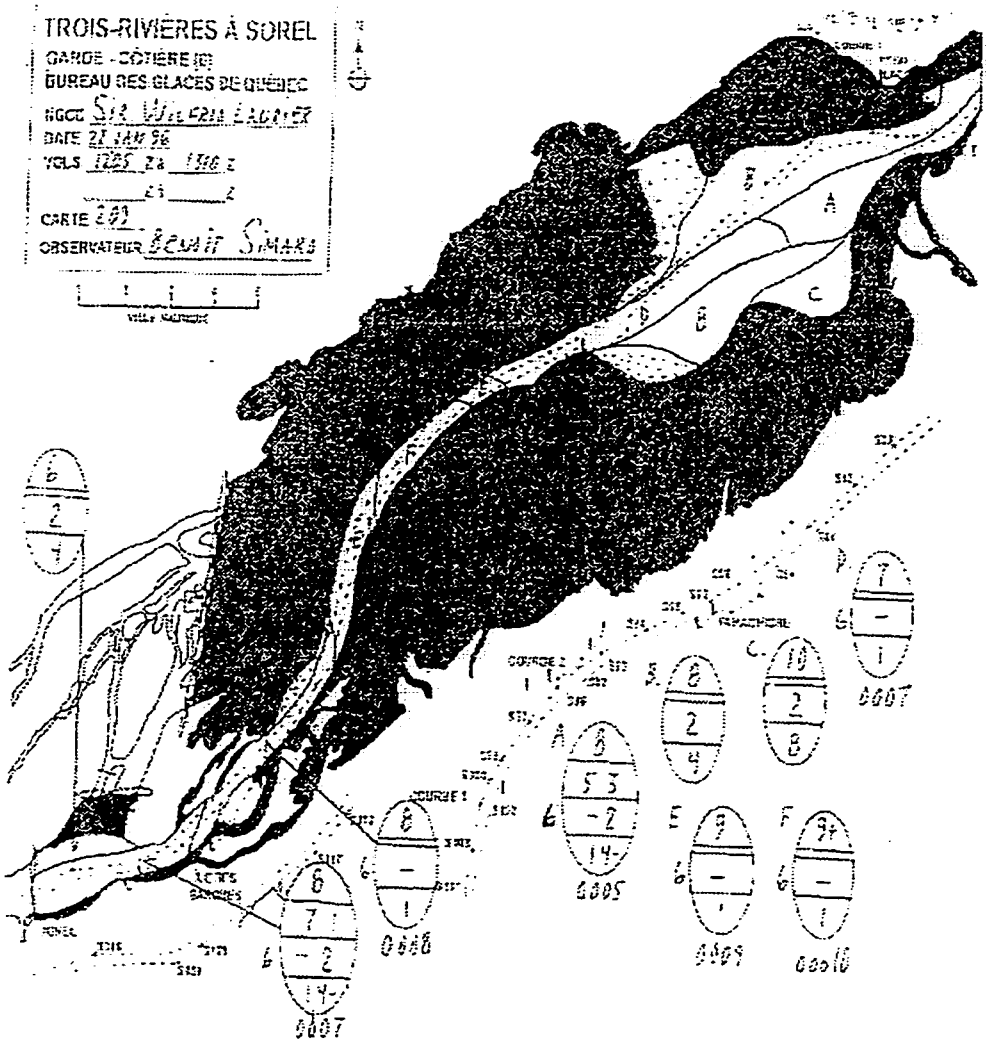

Figure 14: Ice chart of 22 January 1996.

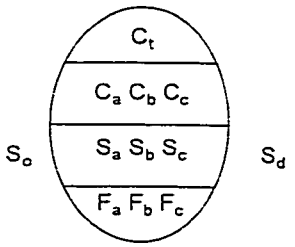

Figure 15: Egg code used in characterising ice.

In addition to ice charts, aerial surveys are made to determine the ice edge location. The location of the ice edge is then accurately drawn on a map of the lake, providing a more complete and accurate picture of the ice conditions at that time. An example of an ice edge drawing is given in Figure 16 for January 22nd, 1996.

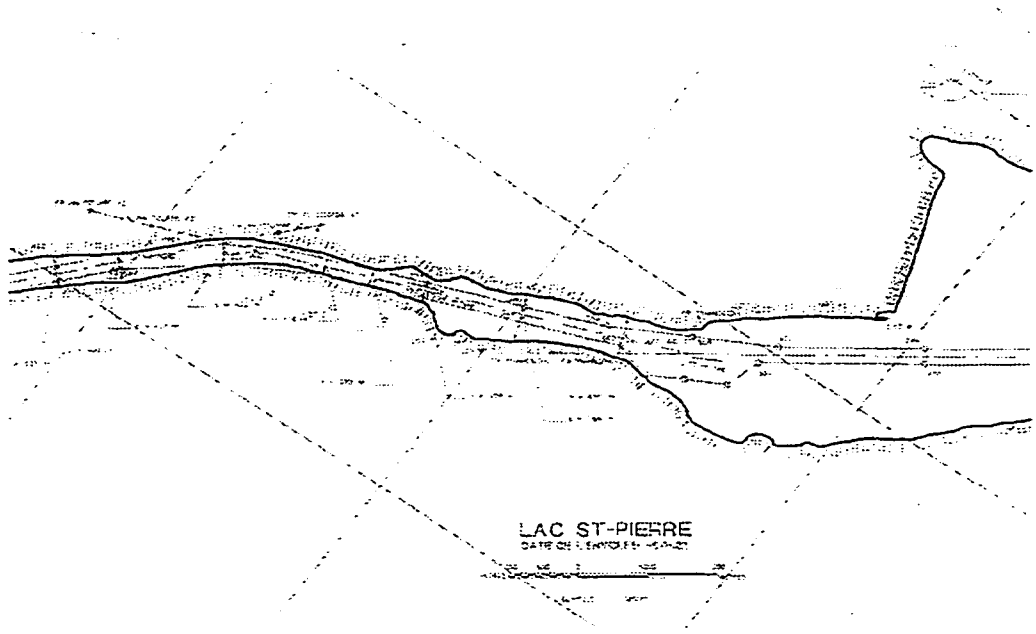

Figure 16: Ice edge for 22 January 1996.

4.2.2 Ice Movement Observations

The ice movements are measured using sonar and camera. While the camera gives a more qualitative information on ice movement, the sonar provides hourly measurements of ice fluxes. The Coast Guard is now working on ways to extract more information from the video image. By adding a grid and calibrating the image, it would be possible, for example, to determine the ice floe size and velocity.

4.2.3 Meteorological Observations

Meteorological data are available from a weather station located at Curve #2, or nearby Environment Canada stations. The Curve #2 station reports hourly air

temperature, wind magnitude and wind direction. An example of wind data for Curve #2 on Lac St-Pierre is given in Figure 17, while Figure 18 show an example of temperature data at that same location.

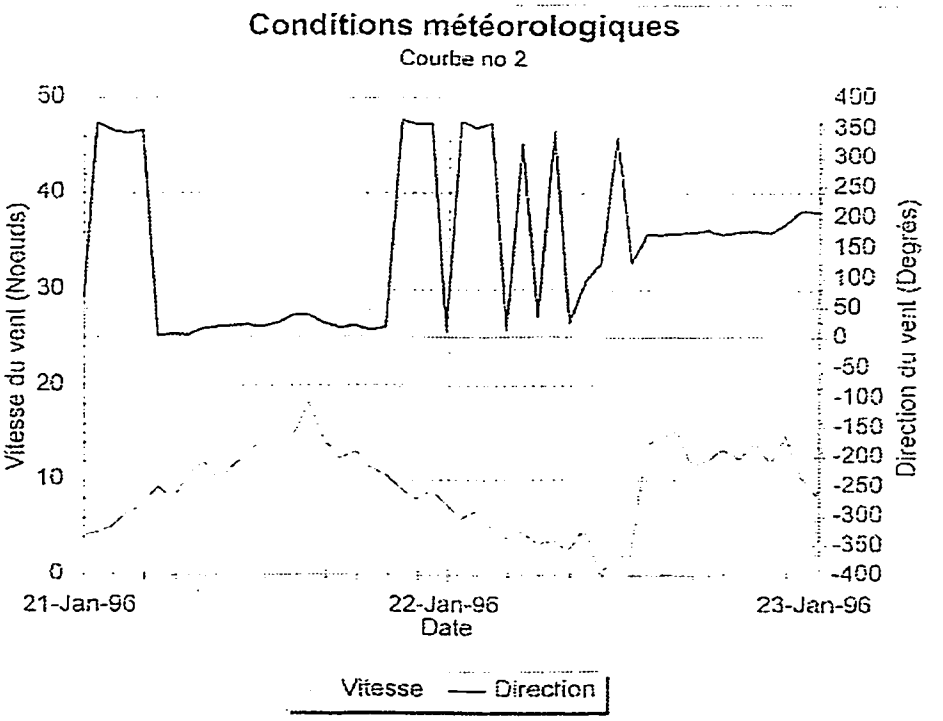

Figure 17: Wind data for 22 January 1996. The left axis and thin line give the wind speed in knots, while the right axis and bold line give the wind direction in degrees.

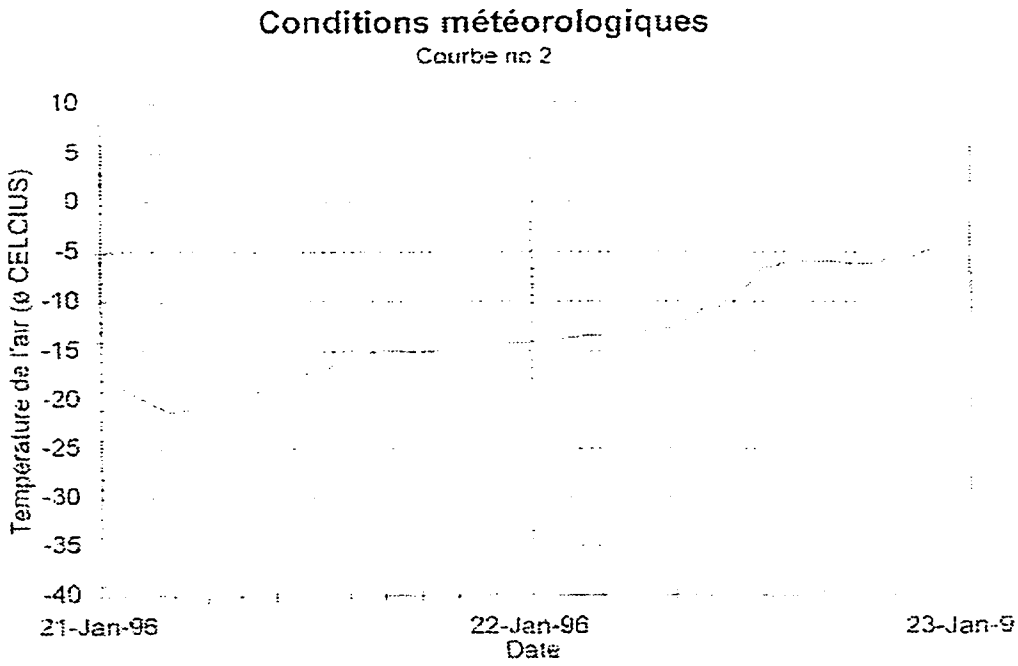

Figure 18: Air temperature data for 22 January 1996.

5 - REVIEW OF PREVIOUS MODELLING STUDIES OF LAC ST-PIERRE

A large amount of data was collected during the first task and presented in previous sections. Part of that data are results of numerical modelling studies conducted at the Canadian Hydraulics Centre in 1994 and 1997 (Sayed *et al*. 1994, Serrer *et al.* 1997). This section will briefly summarise the main findings from these two studies, while the Section 6 discusses additional model simulations that were performed as part of the present study.

5.1 CHC 1994 Study

The objective of this initial effort was to study the transport of ice in Curve 2 of Lac St-Pierre in order to get a better understanding of the processes involved in the formation of ice jams at that location. Sayed, Serrer and Arden (1994) used the Pdyn model (see Section 2.2.2) to simulate ice movement in the Curve under various conditions.

A total of 19 runs were performed with variables selected to examine the role of the following factors:

- Smoothing of the transition between Curve 2 and the straight channel;
- Influence of the channel width;
- Influence of water currents;

- Influence of wind magnitude and direction;
- Impact of an obstruction downstream from Curve 2; and
- Impact of a single large floe in Curve 2.

A simplified representation of the shipping channel around Curve 2 in Lac St-Pierre was used. The channel geometry comprised a straight reach followed by a curve. The values of the ice concentration, velocity and flux were calculated for two cross-sections of the shipping channel. The first section was located in the straight reach, while the second section is taken inside Curve 2. Various scenarios were simulated, with model conditions as presented in Table IV, with the "baseline conditions" represented by simulation number 34. In this table, the shaded values represent parameters that were varied from the baseline conditions. In addition to varying the ice concentration, current, and wind conditions, the study looked at the impact of the curvature of the channel. A limited number of simulations, identified as "blocked" exit conditions in the Table, were performed with fixed particles placed at the exit of the curve to simulate a partial obstruction of the channel. Others were performed with larger floes placed at the North or South of the channel, or using generally smaller floes.

Table IV: Test matrix for CHC 1994 study.

Test Matrix								
No	Channel width (m)	Initial ice concentration	Water current (m/s)	Wind direction	Wind magnitude (knots)	Exit conditions	Curvature	Comments
34	244	0.64	0.5	-	0	free	normal	
35	244	0.75	0.5	-	0	free	normal	
36	244	0.75	0.5	NE	15	free	normal	
37	244	0.64	0.5	NE	15	blocked	normal	
38	244	0.64	0.5	-	0	blocked	normal	
39	244	0 64	0.5	E	15	blocked	normal	
41	244	0.75	0.5	-	0	free	normal	Large floe on North side
42	244	0.75	0.5	-	0	free	normal	Large floe on South side
1	244	0.75	0.5	-	0	blocked	smooth	
1a	244	0.75	0.5	-	0	free	smooth	
2	244	0.75	0.5	-	0	blocked	normal	with 15 diameter blockage
3	274	0.75	0.5	-	0	free	normal	
3a	213	0.75	0.5	-	0	free	normal	
4	244	0.75	0.7	-	0	free	normal	
5	244	0.75	0.5	-	0	free	normal	Floes 25% smaller
9	244	0.75	0.9	-	0	free	normal	
10	244	0.75	0.5	-	0	free	normal	Variable water current
11	244	0.75	0.3	-	0	free	normal	

While most factors considered had some impact or another on ice transport, results of the study mostly demonstrated the large impact of the channel plan-form geometry and channel width on the ice flux predicted by the model. Results showed that a smoother transition between Curve 2 and the straight channel

increased the average ice flux from 50 m^2/s to 60 m^2/s, while ice velocity remained more or less the same. The impact of the channel width was also important with an increase in ice flux in the order of 30% when the channel width was increased from 244 m to 274 m. A reduction in the channel width was found to decrease the ice flux by about the same percentage.

This first application of the Pdyn model to Lac St-Pierre showed the model's ability to provide accurate estimates of ice transport inside the shipping channel and to quantify the impact of various factors on the ice clearing capacity of the channel.

5.2 CHC 1997 Study

A second modelling study was carried out in 1997 by CHC, again using the Pdyn model (Serrer *et al.*, 1997). This second set of simulations was performed using more complex channel geometries corresponding to the actual ice edge maps of Lac St-Pierre for January 19, January 22, and February 14, 1996.

At its narrowest point, the channel had a width of 218 m. Ice floe size were varied between 18 m and 30 m, with an initial ice concentration around 95%, although ice concentration was found to adjust itself to lower values once the ice started moving. A total of 8 runs were performed with a variety of environmental/flow conditions. The water current field was obtained from an existing numerical model of the area and was therefore not uniform across the

channel width. The results revealed that the ice flux is mostly dependent on the water current. For the range of conditions tested, no ice jam formed in the channel.

6 - NUMERICAL MODELLING OF ICE TRANSPORT: METHODOLOGY

6.1 Description of CHC's Pdyn Model

The Pdyn model was developed at the Canadian Hydraulics Centre of the National Research Council by Dr. M. Sayed. Its mathematical approach is described in Section 2.2.2. The ice is modelled as discrete circular particles that are displaced as a result of forces due to current, wind drag and inter-particular contacts. The position and descriptive parameters of each particle are calculated at each time step of the simulation. The Pdyn model provides an accurate representation of ice movement and has been applied to Lac St-Pierre in two studies presented in Sections 5.1 and 5.2.

The Pdyn model set-up, processing and post-processing are relatively simple, but time-consuming. Once set-up, a typical 2-hour simulation with approximately 5000 particles takes around 6 hours to complete on a PentiumPro 200 MHz PC. This relatively long processing time makes the run-time version of the model unsuitable for integration within an ice management system. However, results of model simulations can still provide a very valuable basis for the development of either quantitative relationships, or of a table that could in turn be used within an

integrated ice management tool. It is with this objective in mind that the simulations were carried out.

6.2 Test Program

Three main channel configurations were simulated. These configurations correspond to simple shapes that can be combined to represent what is most commonly observed in the field. Figure 19 shows the three main channel configurations: straight channel, curved channel, and channel with a convergence (funnel).

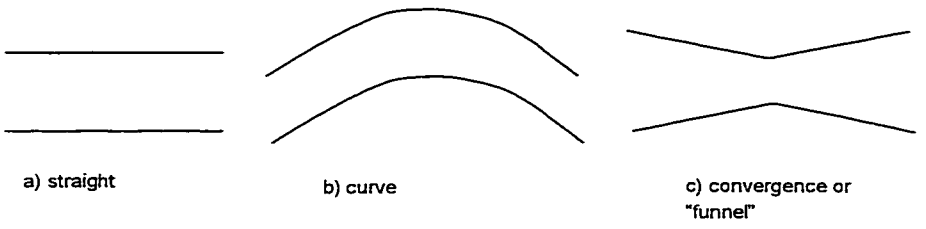

Figure 19: Channel configurations simulated.

In the case of the straight channel, a total of five different channel widths were simulated: 180 m, 210 m, 240 m, 270 m, and 300 m. These widths represent the range of conditions that can be expected on Lac St-Pierre during winter months. The nominal width of the shipping channel is 240 m.

For both the curve and constriction configurations, two sub-categories were considered. Two curvatures were defined: sharp and smooth curves. The sharp

curve had an approach angle of 25 degrees, while the smoother curve had an approach angle of 10 degrees. In the case of channels with a constriction, two different convergence angles of 2.5 and 5 degrees were considered, corresponding to width reductions of 0.087 m/m and 0.175 m/m, respectively.

Figures 20 to 22 show the three main channel configurations and present snapshots of the channel at the end of three representative runs.

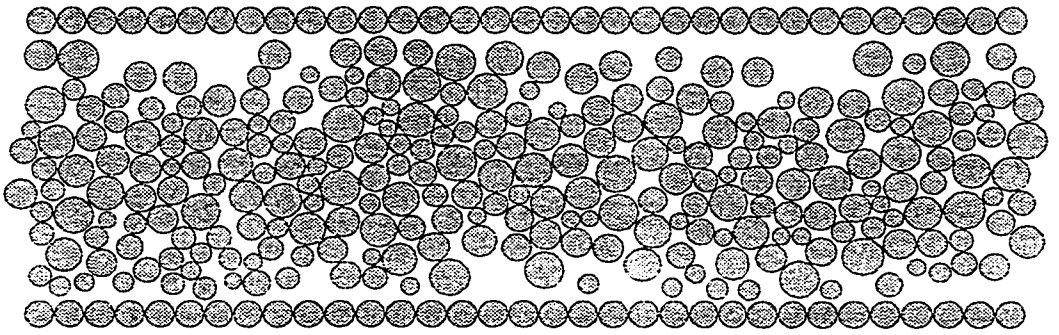

Figure 20: Snapshot at the end of the simulation with straight channel, 0.7 m/s water current.

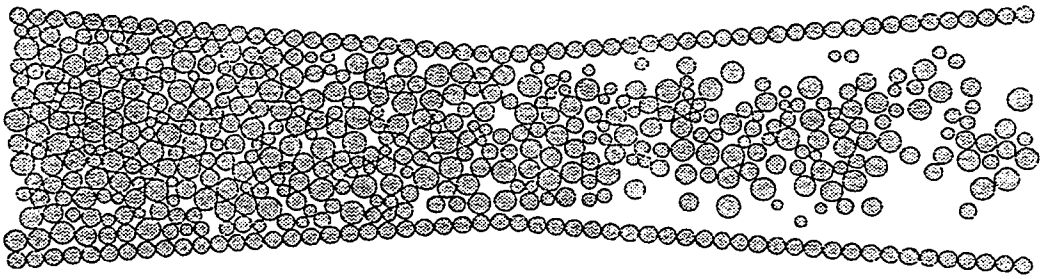

Figure 21: Snapshot at the end of the simulation with funnelled channel (constriction), 0.7 m/s water current.

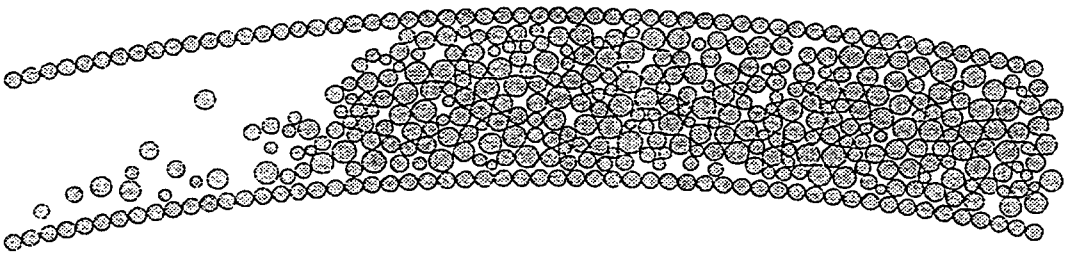

Figure 22: Snapshot at the end of the simulation with curved channel, 0.7 m/s water current.

Wind conditions in the area vary greatly. However, some wind directions and magnitudes are known from experience to promote congestion in the channel, especially winds from the Northeast, opposite to the water current. The various combinations to be simulated were identified as:

- Adverse winds from the NE (10, 15 and 20 knots);
- Winds at 45° from the N and E (10, 15 and 20 knots);
- Intermediate winds from the NNE and S; and
- Favourable winds from the SW (10 knots);

The influence of ice concentration, thickness and size was also studied. Ice floe diameter was assigned randomly between specified minimum and maximum values. A normal distribution of radii varying from 7.5 m to 17.5 m was used as the base case, which results in a mean floe diameter of 25.0 m. This diameter corresponds to small first-year floes. Two other floe size distributions were used for a few simulations with mean floe diameter of 20.0 m and 30.0 m, respectively.

Ice thickness affects the shear resistance at the air and water interfaces. The ice thickness was varied from 0.35 m to 1.0 m, with most of the runs carried out with ice thickness of 0.50 m.

Ice concentration was varied for the different configurations by randomly removing particles from the channel when packed at its maximum. The maximum concentration was approximately 0.80 for the different channel configurations, and ice concentrations as low as 0.55 were considered.

A total of 94 runs were performed. A summary of the various simulations conditions is presented in Appendix A.

6.3 Definition of Parameters

The Pdyn numerical model outputs, at each time step, the position and velocity of each ice particle. Some of the values obtained are:

- $X_{i\,t}$ X-coordinate of particle i at time t.
- $Y_{i\,t}$ Y-coordinate of particle i at time t.
- $Vx_{i\,t}$ X-component of the velocity of particle i at time t.
- $Vy_{i\,t}$ Y-component of the velocity of particle i at time t.

Figure 23 shows a schematised snapshot of a section of the channel at a given point of time. Some parameters are defined on that figure.

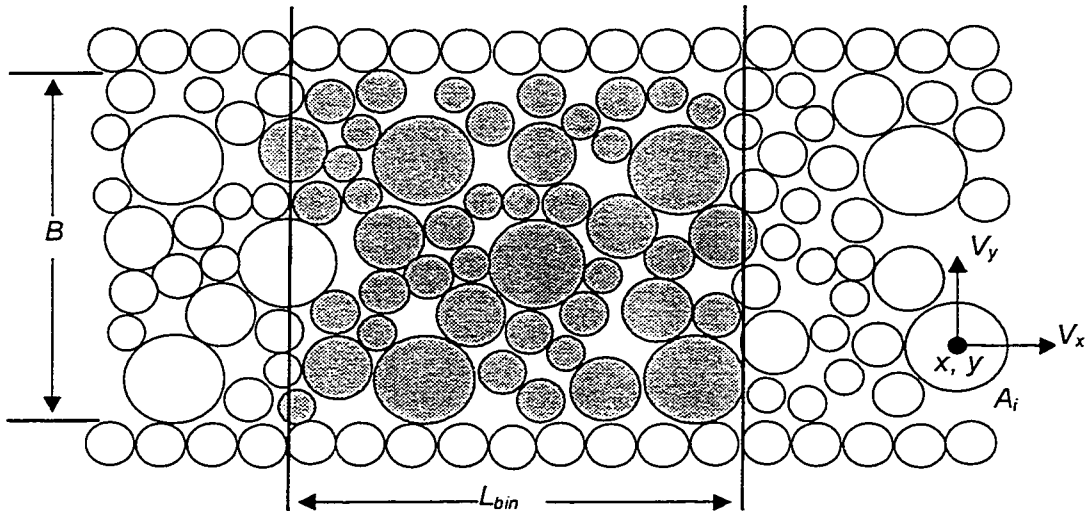

Figure 23: Schema of simulated ice transport.

The simulation results were processed to calculate, at each time step, and at given locations along the channel, the ice concentration, ice velocity, and ice flux. These parameters are defined as:

Ice concentration:

$$(25.) \quad C_{ice} = \frac{1}{B \times L_{bin}} \sum_{i=1}^{p} A_i$$

where A_i is the area of particle i, p is the number of particles located within the specified bin or "sections" (shaded in Figure 23), and L_{bin} is the length of that bin (in the X direction). A bin is defined by a region delimited by given X and Y coordinates.

Ice velocity V_{ice} (m/s):

$$(26.) \quad V_{ice} = \frac{1}{p}\sum_{i=1}^{p} Vx_i$$

where Vx_i is the instantaneous velocity of particle i.

Ice flux F_{ice} (m^2/s):

$$(27.) \quad F_{ice} = \frac{1}{L_{bin}}\sum_{i=1}^{p} A_i \times Vx_i$$

The ice flux is expressed in m^2/s. Volumetric flux of ice transiting through a given section would be obtained by multiplying F_{ice} by the ice thickness h_i.

The simulations output was processed to extract instantaneous ice concentration, velocity and flux at each time step for a given number of specified bins. Time series of the ice concentration, velocity and flux were therefore obtained, examples of which are presented in Figures 24 to 26. In these figures, Sections 1, 2 and 3 are taken at three different locations along the channel, progressing downstream with the flow.

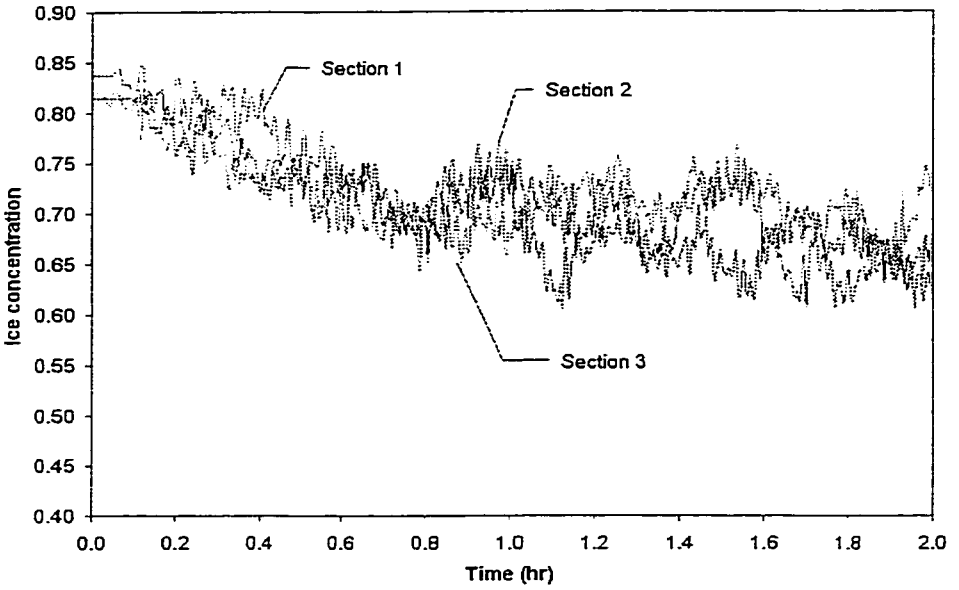

Figure 24: Time series of ice concentration, straight channel 240 m wide, no wind, 0.5 m/s current.

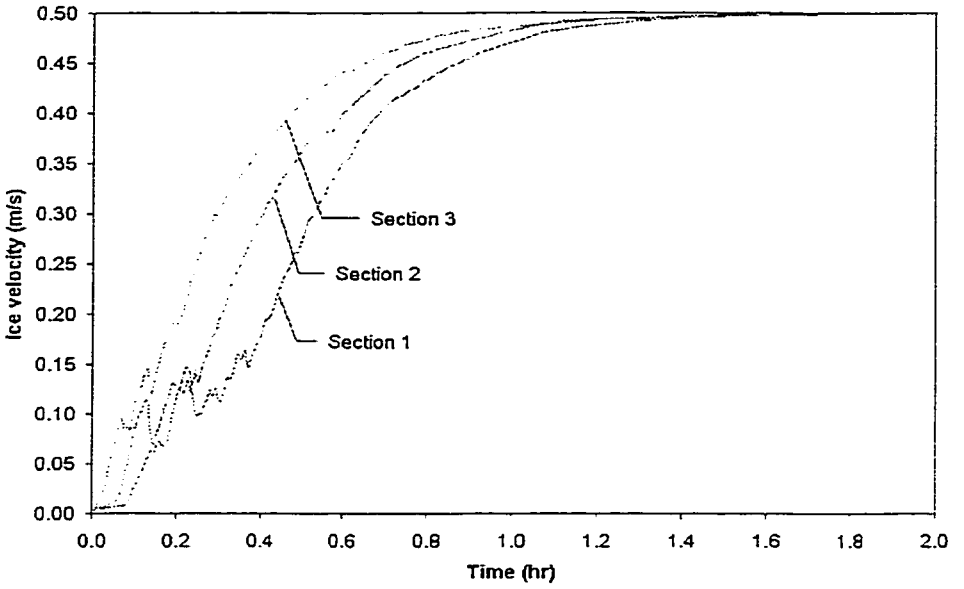

Figure 25: Time series of ice velocity, straight channel 240 m wide, no wind, 0.5 m/s current.

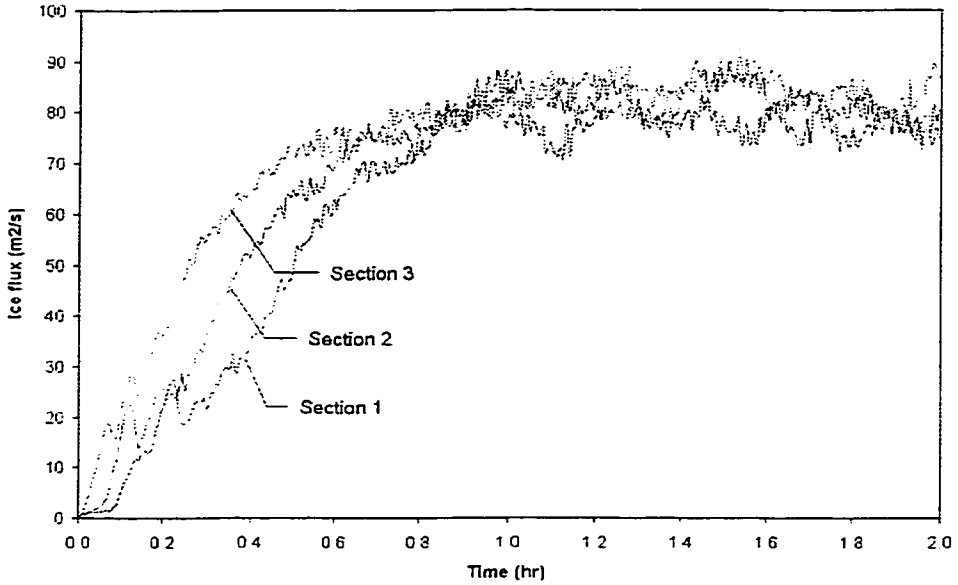

Figure 26: Time series of ice flux, straight channel 240 m wide, no wind, 0.5 m/s current.

As we can see from these figures, it takes a certain time for the ice to start moving and reach a certain "steady-state" level after approximately one hour. The average, minimum and maximum values of the ice concentration, velocity and flux were calculated for the period between 1.0 and 2.0 hours. These reduced statistical parameters were used for comparing the results of the various simulations.

When comparing results of simulations performed with different water current and/or channel width values, the ice velocity and flux were "normalised" using the following definitions:

(28.) $$V_n = \frac{V_{ice}}{u}$$

(29.) $$F_n = \frac{F_{ice}}{uB}$$

where u is the water current velocity (m/s).

7 - NUMERICAL MODELLING OF ICE TRANSPORT: RESULTS

The results from the Pdyn simulations were analysed to determine the impact of various factors on ice velocity and flux. The variables considered were the channel width and geometry, wind direction and magnitude, water current, and ice concentration and thickness.

7.1 Channel Width

Four channel widths were simulated: 210 m, 240 m, 270 m, and 300 m. As could be expected, the width of the channel has a very strong influence on the ice velocity and flux. Figure 27 presents the average measured ice velocity for simulations with different water current and channel widths, while Figure 28 presents the average measured ice flux.

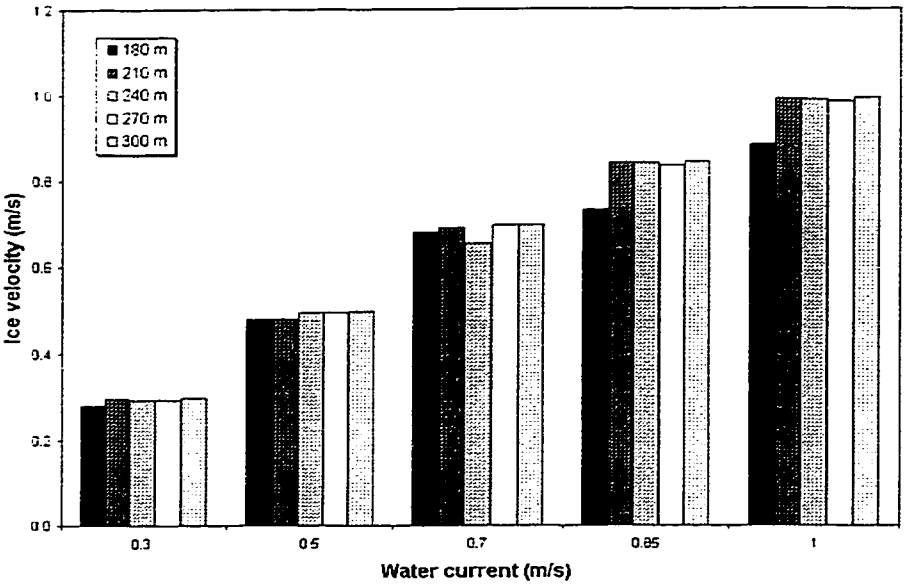

Figure 27: Influence of the channel width on average measured ice velocity, straight channel.

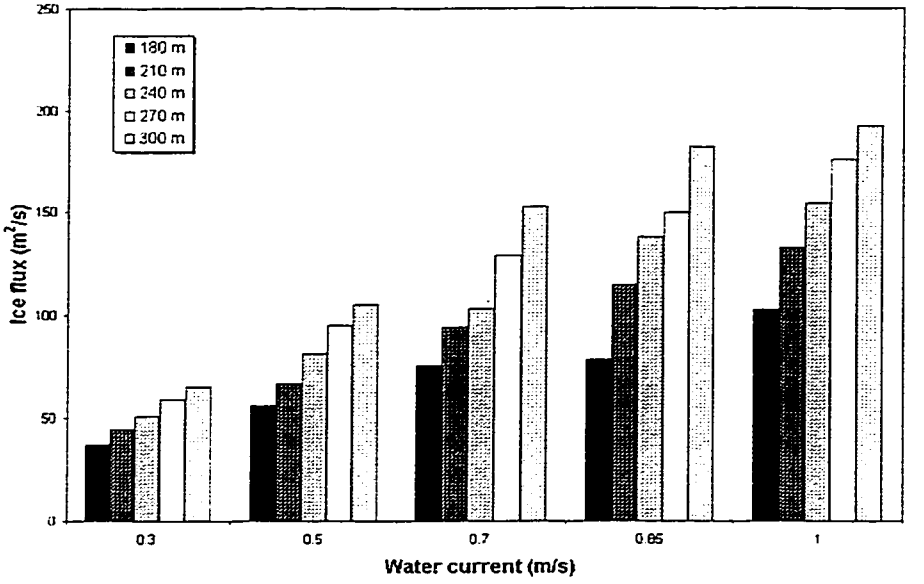

Figure 28: Influence of the channel width on average measured ice flux, straight channel.

As we can note from Figure 28, the impact of the channel width on the ice flux is quite substantial. This could be expected, considering how the ice flux is defined. In order to isolate the influence of the channel width on ice movement, normalised values for the ice velocity and flux were defined as a function of the ambient current velocity. The impact of channel width on the normalised ice velocity (V_{ice}/u) is shown in Figure 29. Normalised values under 1.0 mean that ice is moving slower than the water current.

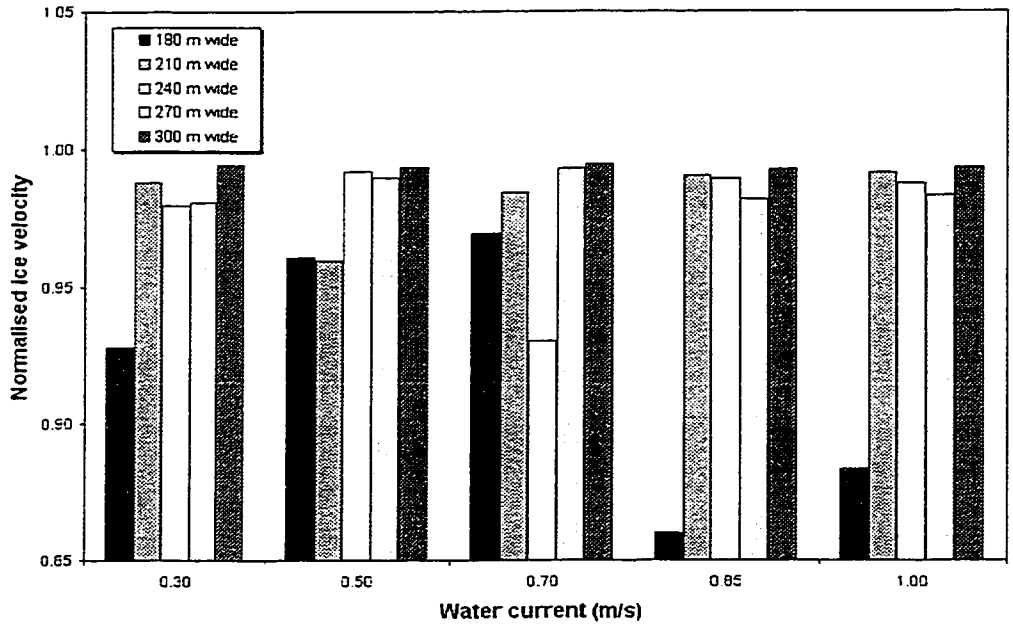

Figure 29: Influence of channel width on the normalised ice velocity, straight channel, no wind.

Figure 30 presents the same information differently where the effect of the channel width is emphasised.

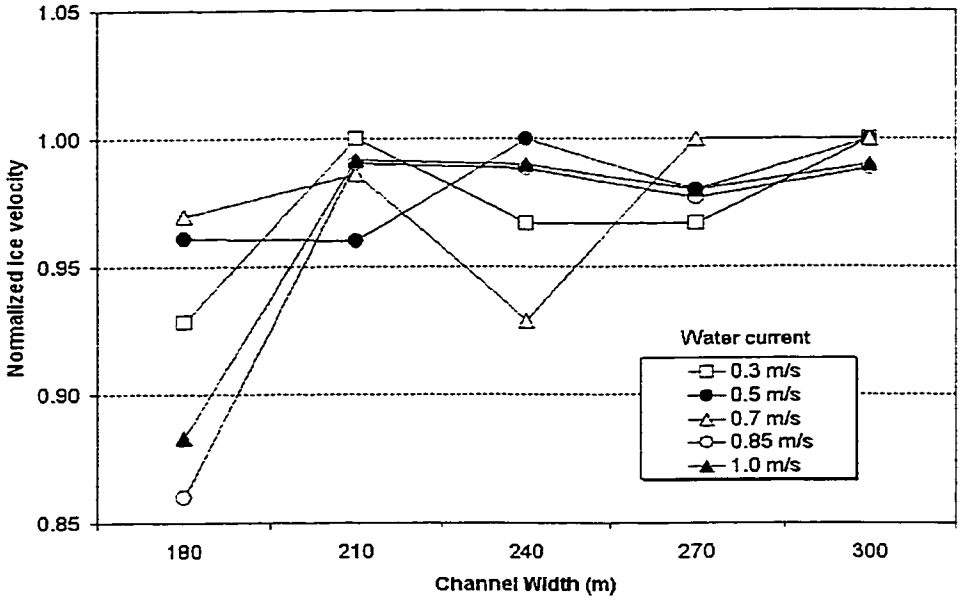

Figure 30: Influence of channel width on the normalised ice velocity.

As we can note from the two figures above, the ice velocity becomes much smaller than the driving water current as the channel width is reduced. This is mostly due to the higher influence of the bank resistance to ice movement, as well as the higher ice diameter to channel width ratio, which increases inter-particular contact.

Figure 31 presents the influence of the channel width on the normalised average ice flux. Again, there is a general tendency for the normalised ice flux to increase as the width of the channel increases.

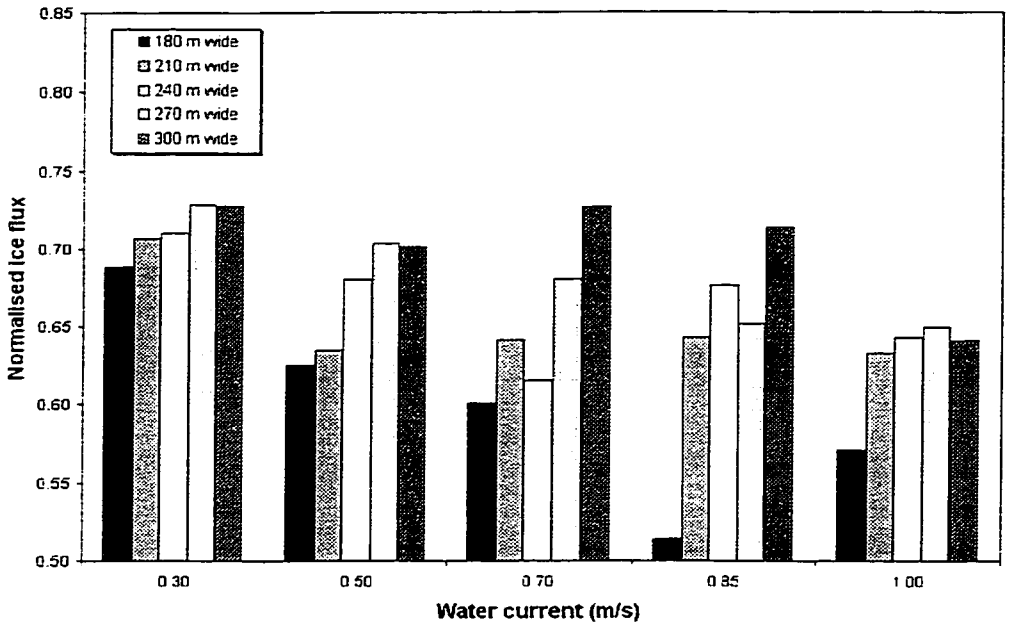

Figure 31: Influence of channel width on the normalised ice flux, straight channel, no wind.

7.2 Channel Geometry

Three main channel geometries were simulated: straight, curve and funnel. The curve and funnel channels were further subdivided into smooth and steep transitions. Figure 32 and Figure 33 present the impact of the various channel shapes on ice velocity and flux, respectively

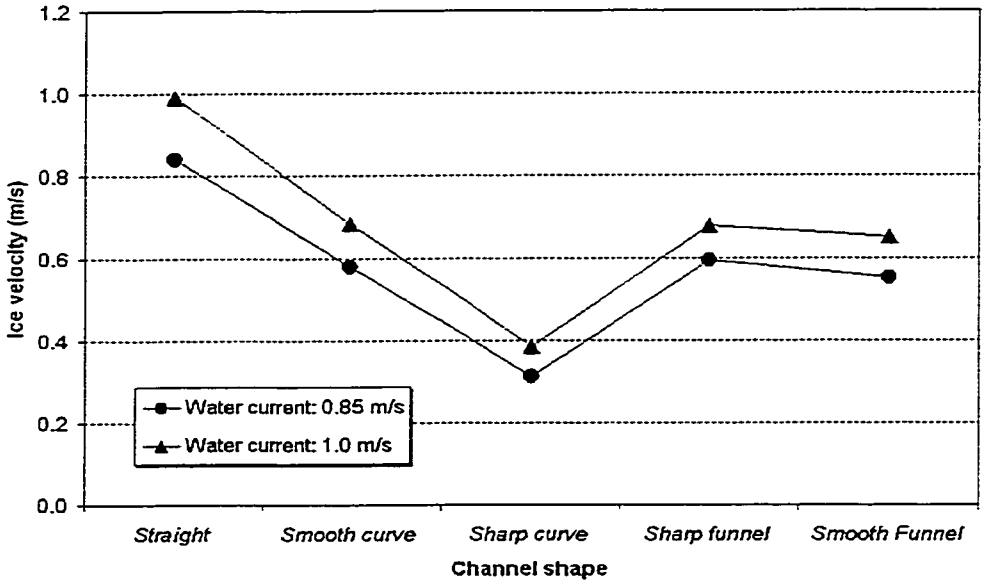

Figure 32: Influence of channel shape on ice velocity for water currents of 0.85 m/s and 1.0 m/s.

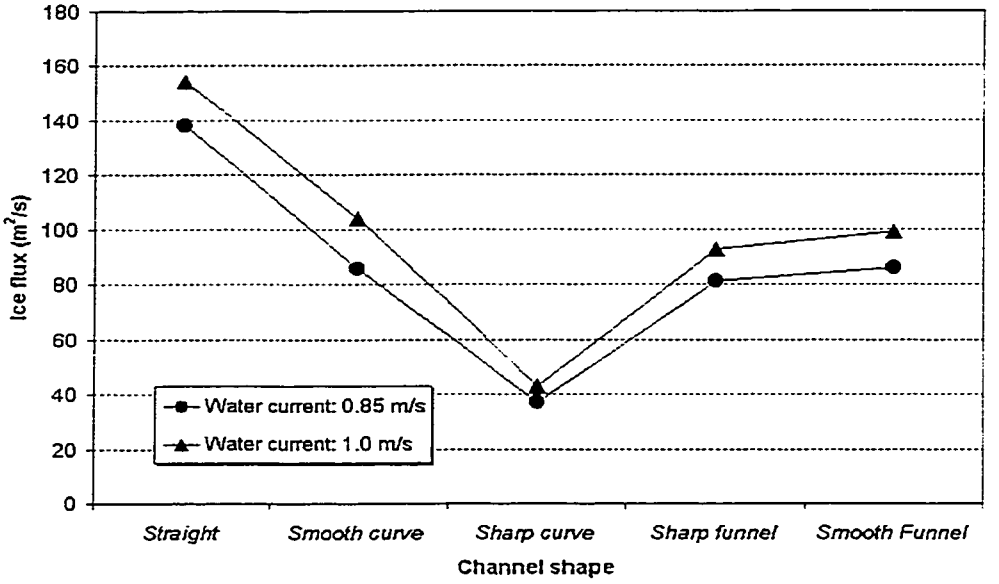

Figure 33: Influence of channel shape on ice flux for water currents of 0.85 m/s and 1.0 m/s.

As can be noted on these figures, the channel geometry has a very strong impact on both the ice velocity and flux, and hence on its ice clearing capacity. Although all the configurations have a channel width of 240 m at their narrowest point, the actual plan shape of the channel greatly affect circulation of the ice. The drop in both the ice velocity and flux is in the order of 70% when comparing curved channels with straight ones. The drop is less pronounced between constriction (funnel) and straight channels, i.e. in the order of 35%.

7.2.1 Channel with constriction (funnel)

The ice movement in a channel with a constriction is strongly affected by the severity of the width reduction and by the width of its narrowest section. The ice velocity and flux on the upstream side of the constriction are reduced, as the particles must pass through the narrower section. Once the narrower section is cleared however, the ice velocity and flux increase again.

Figure 34 presents the ice velocity as a function of the water current for sections before, within, and after the constriction. Figure 35 presents the corresponding ice fluxes. Sections 1, 3 and 5 are located upstream, at the narrowest point, and downstream of the constriction, respectively. Note that the figures below show that the clearing capacity of a channel with a "funnel" geometry is limited by the capacity of the portion upstream from, or at its narrowest section.

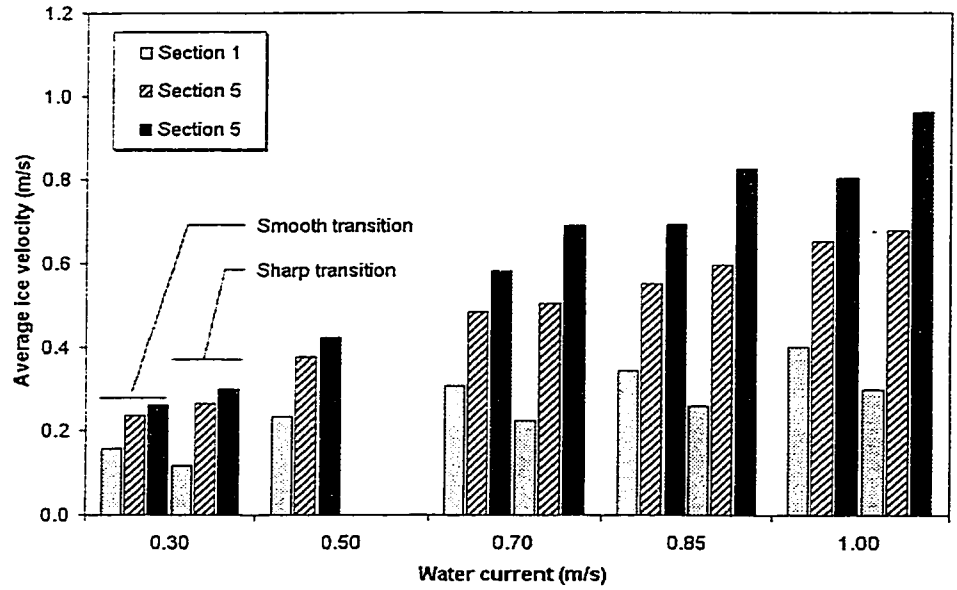

Figure 34: Ice velocity for funnelled channels, soft and sharp transitions, no wind.

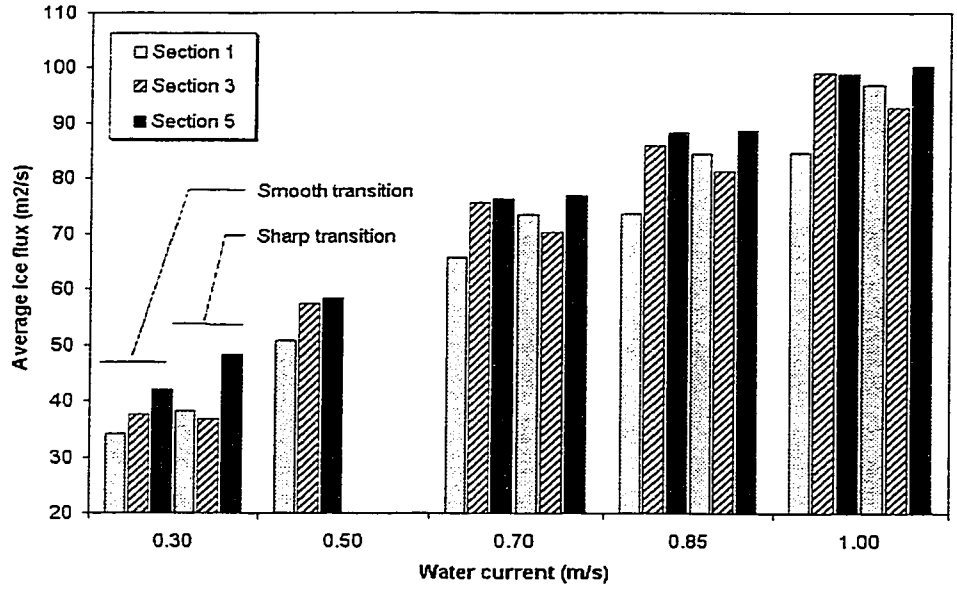

Figure 35: Ice flux for funnelled channels, soft and sharp transitions, no wind.

7.2.2 Curved channel

Similar to funnel channels, where ice clearing is a function of the severity of the constriction, the ice movement in a curved channel is affected by the channel's curvature. The sharper curvature means lower ice velocities, both before, within, and after the curve. In general, the ice velocity inside the curve is reduced compared with upstream and downstream velocities. Ice flux follows the same trend. The overall ice clearing capacity of a channel presenting a curve is therefore limited by the capacity of the curve itself. This is illustrated in the following figures where Figures 36 and 37 respectively show the ice velocity and flux for the various configurations. In these figures, Section 1 is located upstream of the curve, Section 3 at its apex, and Section 5 is located downstream from the curve.

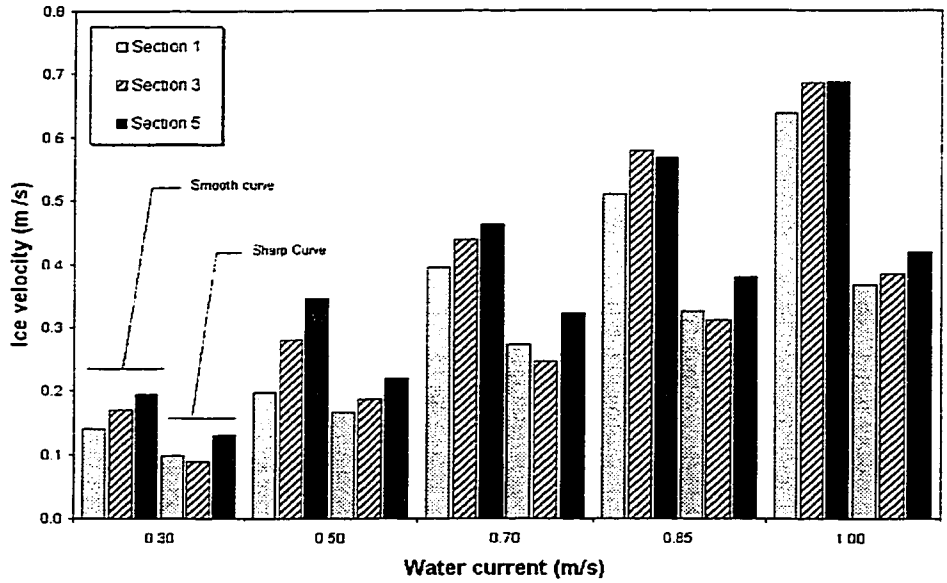

Figure 36: Distribution of the average ice velocity in curved channels, no wind.

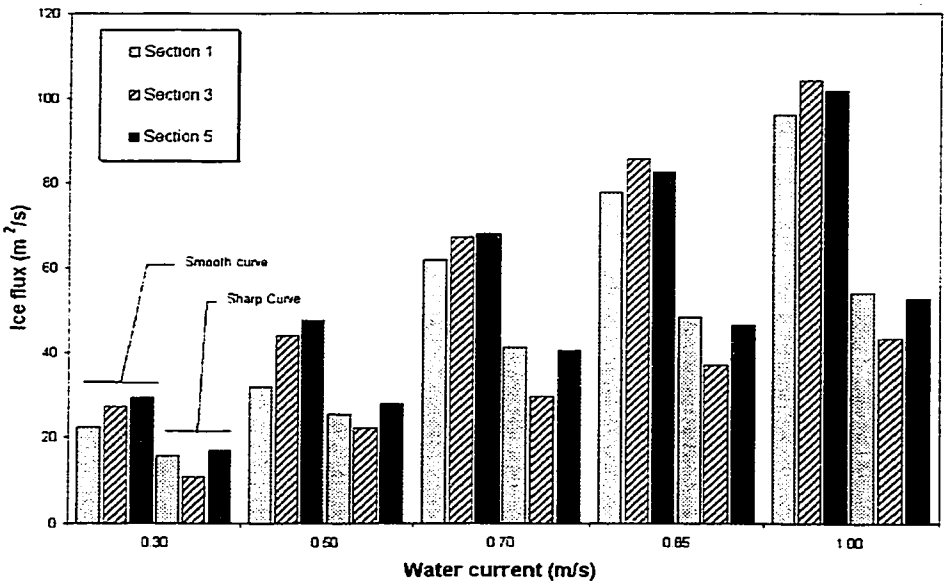

Figure 37: Distribution of the average ice flux in curved channels, no wind.

7.3 Wind

Simulations were performed using different wind directions and magnitudes. Both direction and magnitude were combined to define a single scalar parameter that represents wind resistance to ice movement. This parameter is defined as:

(30.) $$W = V_{wind} \cos(\theta)$$

where V_{wind} is the wind magnitude in knots, and θ is the angle between ambient water current and wind direction, measured counter-clock wise.

Although cross-winds are expected to have a marked effect on ice transport in the channel, such as concentrating the ice on one of the banks, the present series of simulations only considered wind directions differing from current direction by up to 45 degrees.

The impact of the wind on ice velocity and flux is illustrated in Figure 38. As can be noted on that figure, an adverse wind of 15 knots from the NE essentially stops the ice in the channel. This is supported by field observations discussed in Section 3.1.2. On the other hand, a wind of 10 knots blowing in the direction of the water current promotes higher ice velocity and increases the channel's clearing capacity. The increase in ice velocity is quite important, i.e. in the order of 50%. Figure 39 presents the changes in ice velocity by wind direction and magnitude, compared with "no wind" conditions. Percent increase/diminution in the ice velocity are included with positive values indicating an increase.

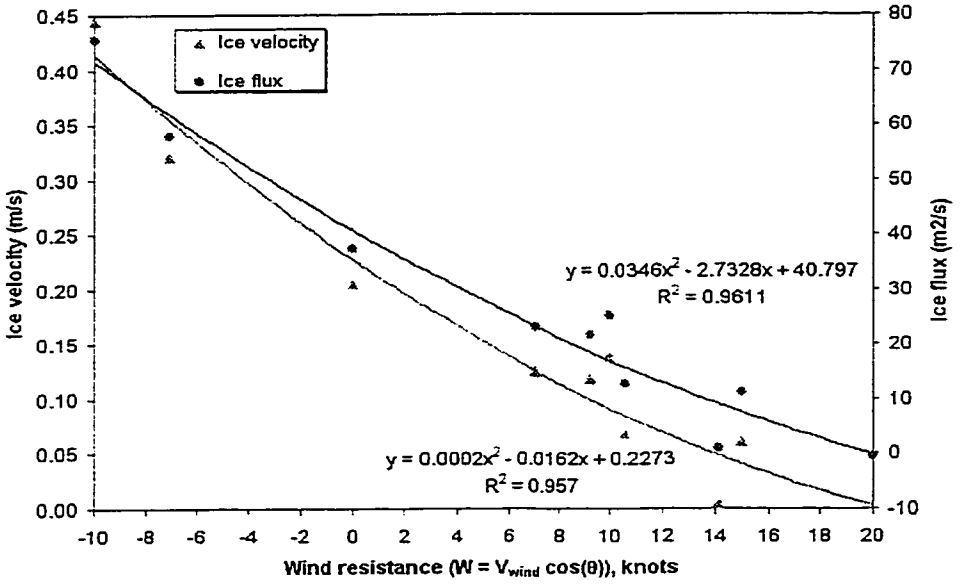

Figure 38: Influence of the wind resistance on normalised ice transport in a straight channel 240 m wide, water current of 0.3 m/s.

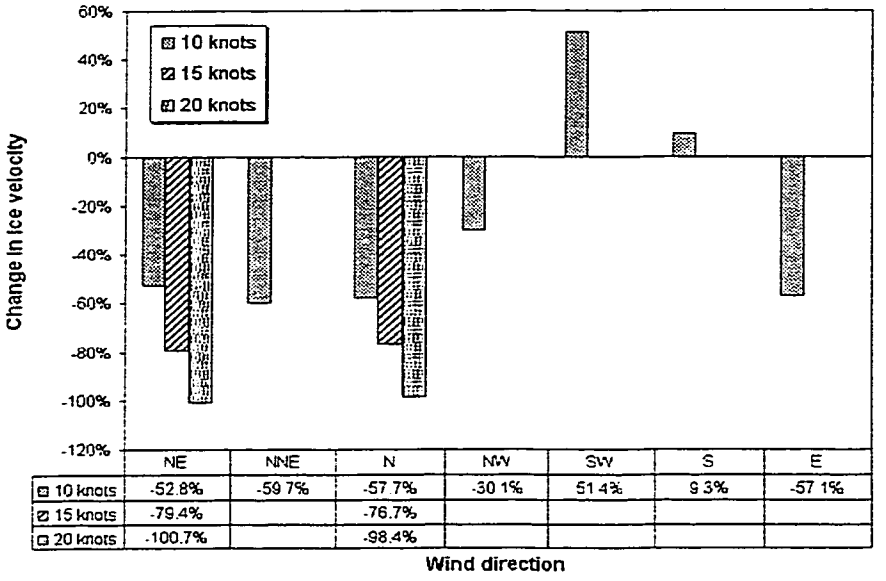

	NE	NNE	N	NW	SW	S	E
10 knots	-52.8%	-59.7%	-57.7%	-30.1%	51.4%	9.3%	-57.1%
15 knots	-79.4%		-76.7%				
20 knots	-100.7%		-98.4%				

Figure 39: Influence of wind direction and magnitude on the ice velocity in a straight channel, 240 m wide, water current 0.3 m/s (expressed in terms of the percentage of change from the "no wind" conditions).

7.4 Water Current

As could be expected, the water current has a direct and considerable impact on ice flux and velocity. Water currents varying between 0.15 m/s and 1.30 m/s were simulated. In the case of a straight channel 240 m wide and without wind, the ice velocity closely matches the water current with values in average 4% lower than the water current. This difference is explained by the interactions within the ice field and between the ice and the channel's banks.

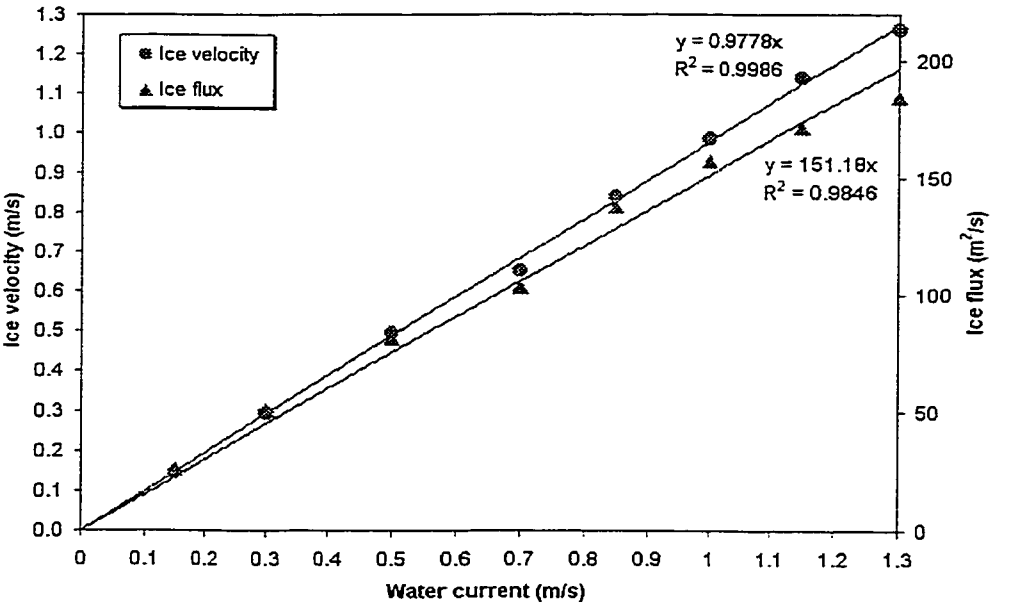

Figure 40: Influence of water current on ice transport in a straight channel, 240 m wide, without wind.

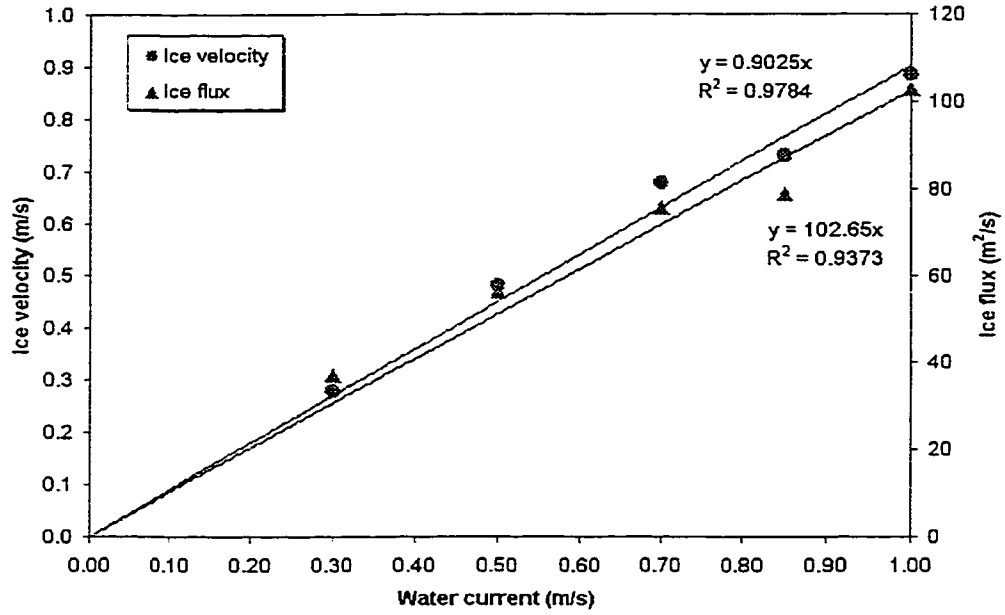

Figure 41: Influence of water current on ice transport for a straight channel, 180 m wide and no wind.

7.5 Ice Concentration

Similar to the water current, the ice concentration has a direct effect on the ice flux and velocity.

Figure 42 presents the influence of the initial ice concentration at the beginning of a simulation on the normalised ice velocity and flux (defined in Section 6.3). As can be noted on that figure, the ice velocity decreases gradually with increasing ice concentration while the ice flux increases. At lower ice concentrations, when interactions within the ice field and with the channel's bank are limited, the ice velocity closely matches the ambient current.

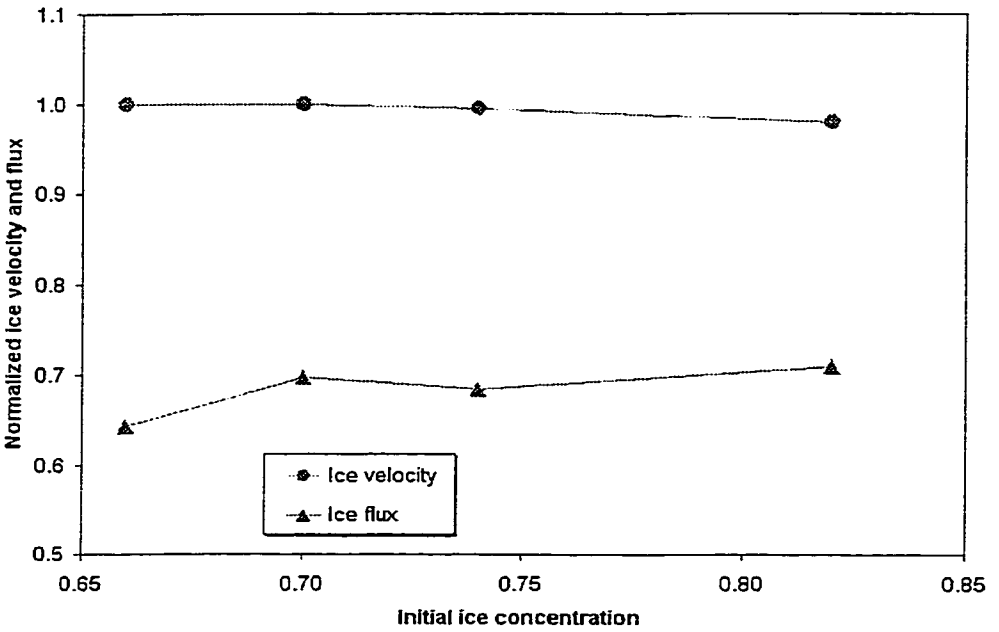

Figure 42: Influence of the initial ice concentration on ice transport, straight channels, no wind.

7.6 Ice Thickness

The thickness of the ice is implicitly specified in the model by adjusting the resistance values of the ice at the air and water interfaces. This resistance is directly proportional to the ice thickness. Simulations were carried out with ice thickness varying from 0.35 m to 1.0 m. Changes in normalised ice velocity and flux with ice thickness are illustrated in Figure 43.

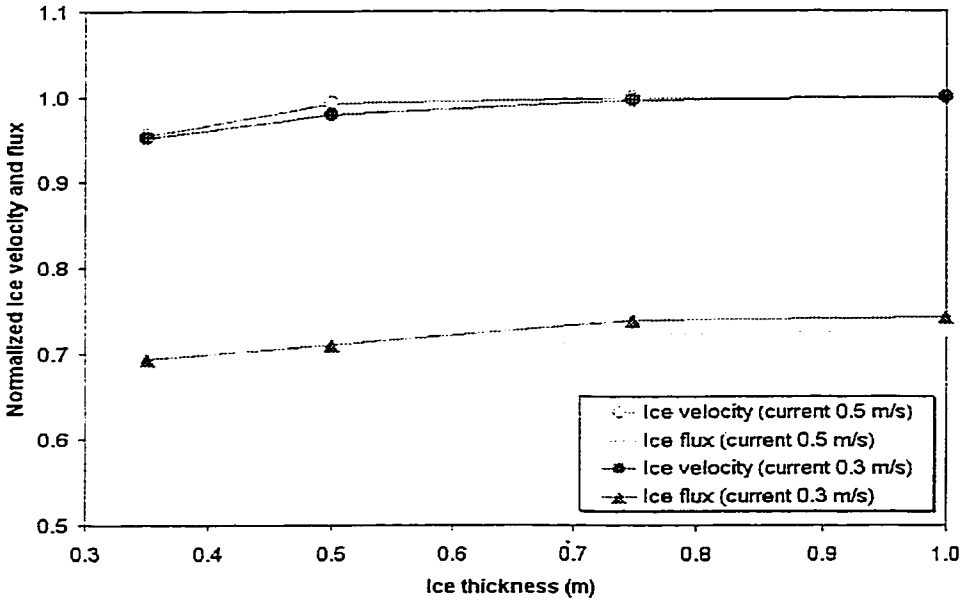

Figure 43: Influence of ice thickness on ice tranport in a straight channel, 240 m wide, without wind.

7.7 Multi-linear Regression

All of the factors presented in Sections 7.1 to 7.6 influence, in one way or another, the ice velocity and flux. However, most of the relationships between these factors and ice transport have been found to be relatively linear. A multi-linear regression analysis was performed to provide insight on their relative importance and to aggregate and formalise the results of the large number of simulation. Multiple linear regression (MLR) is the extension of simple linear regression (SLR) to the case of multiple explanatory variables (Helsel and Hirsh, 1992). The multi-linear regression results in an equation of the first degree that expresses the variable of interest as a weighted sum of the various factors. In our case, the relationships take the following form:

$$(31.) \quad \begin{aligned} V_{ice} &= a_1 + a_2 B + a_3 U + a_4 C + a_5 h + a_6 R + a_7 W \\ F_{ice} &= b_1 + b_2 B + b_3 U + b_4 C + b_5 h + b_6 R + b_7 W \end{aligned}$$

where B is the channel width (in meters), U is the water current (m/s), C is the aerial ice concentration, h is the ice thickness (m), R is the average ice floe radius (m), and W is the wind resistance (knots). The constants $a_1 \ldots a_7$ and $b_1 \ldots b_7$ are regression constants. The following table presents the results of the MLR regression analysis.

Table V: Multi-linear regression constants.

Constant	Ice velocity, V_{ice} (m/s)	Ice flux, F_{ice} (m^2/s)
a1, b1	-0.01753	-123.335
a2, b2	0.000381	0.523064
a3, b3	0.989697	145.0389
a4, b4	-0.17772	-16.7897
a5, b5	0.054585	17.224
a6, b6	0.002153	0.812393
a7, b7	0.015928	2.480792
R^2	0.99	0.98

The regression coefficient R^2 quantifies the goodness of the fit between the equation and the observations. In this case, the fit is almost perfect. Figures 44 and 45 illustrate the comparison between values calculated (from the regression equation) and model results for the ice velocity and ice flux, respectively. The straight line represents a perfect fit (R^2). The values taken by regression constants *a1* through *a7* and *b1* through *b7* give indications as to the correlation between the parameter they are associated with and the ice velocity or ice flux in the

channel. The signs of the regression constants have important significance whereby a negative sign indicate an inverse relationship between the parameter it precedes in Equation 31 and the ice velocity or flux. The magnitude of the constants is also important in determining to what extent the various factors affect the ice velocity or flux, provided that the other parameters remain the same. For example, Equation 31 and the calculated regression parameters indicate that an increase in channel width of 50 meters would result in an increase in average ice velocity of about 0.20 m/s, if all other parameters were to remain the same.

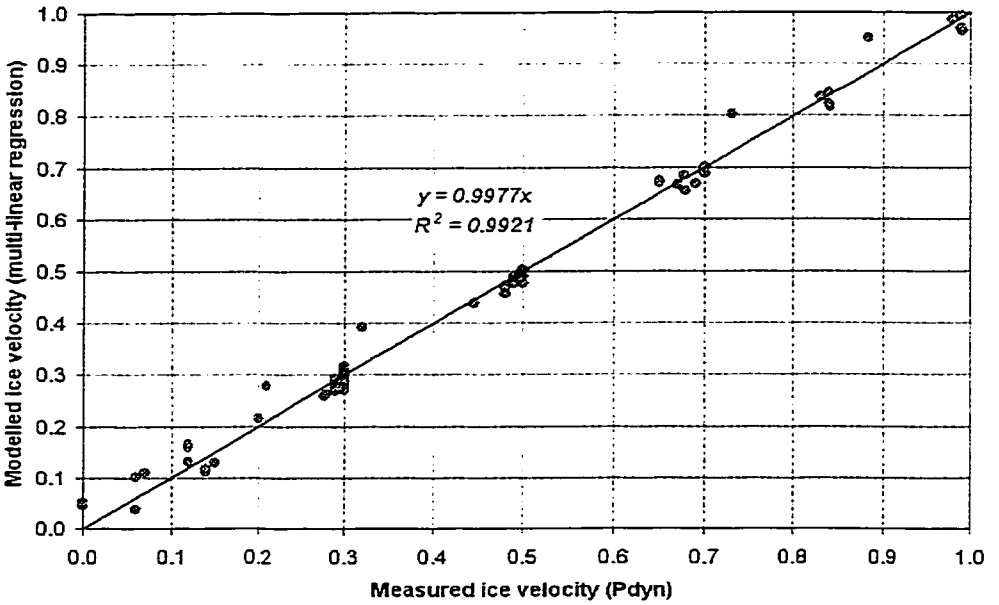

Figure 44: Comparison between ice velocity model results and values calculated from the regression equation.

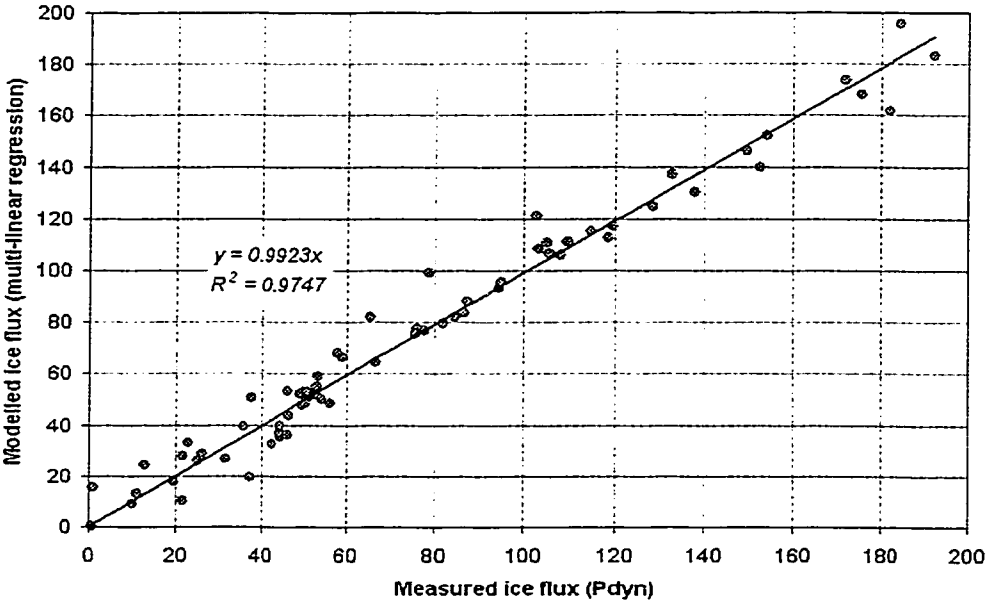

Figure 45: Comparison between ice flux model results and values calculated from the regression equation.

8 - VERIFICATION

The Pdyn simulations results provided extremely valuable quantitative insight on the influence of various factors on ice transport. In order to provide a certain confidence in the predictive capabilities of the relationships obtained, the values obtained using these relationships were compared with those obtained using other existing models.

8.1 Comparison with Ackerman's Equation

The mathematical model proposed by Ackerman was presented in Section 2.2.1. It is composed of a single equation, derived from a large number of numerical simulations, that relates the ice clearing capacity (maximum ice flow) to channel characteristics and environmental conditions.

Assumptions of Ackerman's mathematical model are somewhat different from those for the Pdyn model. While Ackerman's model assumes no interaction of the ice with ice attached to the channel banks, in the case of the Pdyn model, the channel's banks are modelled as fixed ice particles and forces are calculated accordingly on a particle-by-particle basis. The presence of border ice affects the resistance to ice flow and distribution of the velocity across the channel. Ackerman's model is based on the water flow in a straight channel, with regular

cross-section. However, estimation of the flow from the water surface velocity is complicated due to the absence of data on appropriate resistance values.

The Ackerman's model was used to calculate the ice flux for the range of conditions simulated with the model Pdyn. Figure 46 presents the comparison between the Pdyn results and values predicted by Ackerman's model. Since Ackerman's equation does not take into account the effect of the wind, the comparison was done using only "no-wind" conditions.

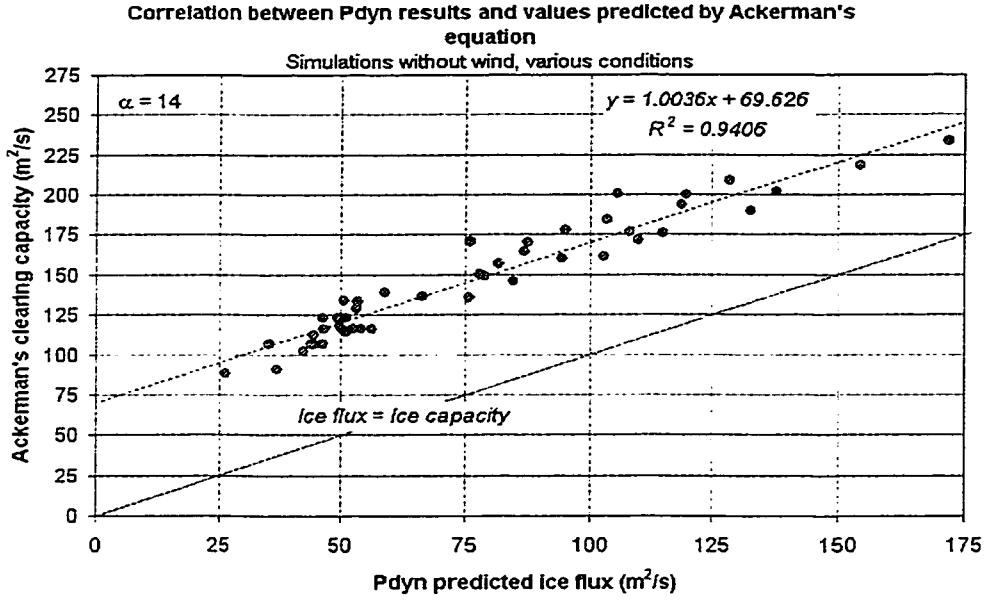

Figure 46: Comparison of values predicted by Ackerman's model and Pdyn results.

As we can see on the figure above, while the slope is consistent with that of a perfect correlation (line labelled "ice flux = ice capacity"), there is a significant offset between the ice flux obtained from the Pdyn model and the value

predicted by Ackerman's model. This difference could be due to a variety of reasons:

- There is a difference in the actual definition of what is being calculated in the two approaches. While the Ackerman model yearns to calculate the highest possible quantity of ice that can be cleared by a given channel under certain conditions, the Pdyn model provides the actual ice flux that would be observed.
- Ackerman's mathematical model strongly depends on the water flow passing in the channel as calculated from a flow-velocity relationship such as Manning's equation. However, some of the important parameters of Ackerman's equation, such as Manning's resistance coefficient n, are difficult to quantify.

The equation derived from Pdyn simulation results presents the advantage, over Ackerman's model, of explicitly taking into account the effect of wind magnitude and direction, which has been shown to be very important.

8.2 Comparison with Sayed's Ice Module

Sayed recently developed an Ice Module as part of Environment Canada Community Ice-Ocean Model (CIOM) (Sayed and Carriere, 1999). The mathematical approach of the Ice Module was presented in Section 2.2.3. While in the Pdyn model the ice is simulated as discrete particles for each of which the net forces are calculated, the CIOM Ice Module calculates advection of discrete

particles and momentum using a mixed Lagrangian-Eulerian approach. The advantage of such a model is its greater calculation efficiency, which allows its use for predictions in quasi-real time.

The Ice Module of the CIOM differs from the Pdyn model not only by the algorithms it uses but also in its input parameters. In the case of the Ice Module, the ice conditions are explicitly defined. The initial ice concentration is specified, which is not the case for the Pdyn model where the ice concentration is the one obtained by packing the channel. The results of two simulations were obtained from Sayed (Personal Communication) and compared with Pdyn results for the same conditions. In both cases, a straight channel of 500 m width was simulated with initial ice concentration of approximately 0.85, and no wind. Ice thicknesses of 0.5 and 1.0 m were used for the two simulations, respectively.

Table VI: Comparison of Pdyn and CIOM Ice Module results.

Model	Ice thickness	
	0.5 m	1.0 m
Initial Average Concentration		
Pdyn	0.702	0.705
CIOM	0.700	0.700
Maximum ice velocity (m/s)		
Pdyn	0.55	0.55
CIOM	0.64	0.51
Maximum ice flux (m^2/s)		
Pdyn	207.7	208.5
CIOM	223.5	176.9

As can be seen from the table above, the maximum ice velocities and fluxes predicted by the CIOM Ice Module differ by no more than 15% from those obtained with the Pdyn model. Although the algorithms and, to a certain extent,

the inputs to the two models are different, the two models are reasonably close in their prediction.

9 - FRAMEWORK FOR INTEGRATION INTO AN ICE MANAGEMENT SYSTEM

9.1 Formulation of the Algorithm

The main findings of the Pdyn simulations were presented in Section 7. The Pdyn model simulations provide very valuable information on factors affecting the ice transport on a channel. Relationships were derived for straight channels that relate the ice velocity and flux to morphological and environmental factors. Effects of the channel shape on the ice transport were also quantified. The curvature of the channel and angle of convergence were found to have a large impact on the quantity of ice that can be cleared by the channel.

How can these relationships and information be used to calculate the ice clearing capacity of a "real" channel as observed on the field? An approach will be suggested in the present section.

The approach rests on calculating the ice clearing capacity of the various sections that compose the channel. The channel is assumed to be a combination of simple geometries, i.e. straight segments, curves and constrictions. The relationships derived for straight channels may be used to calculate the "maximum" ice velocity and flux that would take place in the channel under the specific

conditions, if that channel were straight. This value may then be adjusted for the curves and contractions that are present on the "real" channel.

It is important to remember that the quantity of ice that can be cleared by a given channel depends on the quantity of ice that can be cleared by the most "critical" section along that channel. This was clear in the results of the simulations with funnelled channels. Although the width of the channel was increasing after the narrower section, the flux remained relatively small compared to a straight channel. The influence of the convergence could be felt on a distance that was much longer than the constriction itself. Figure 47 illustrates the position of ice floes in a channel with convergence (funnel shape).

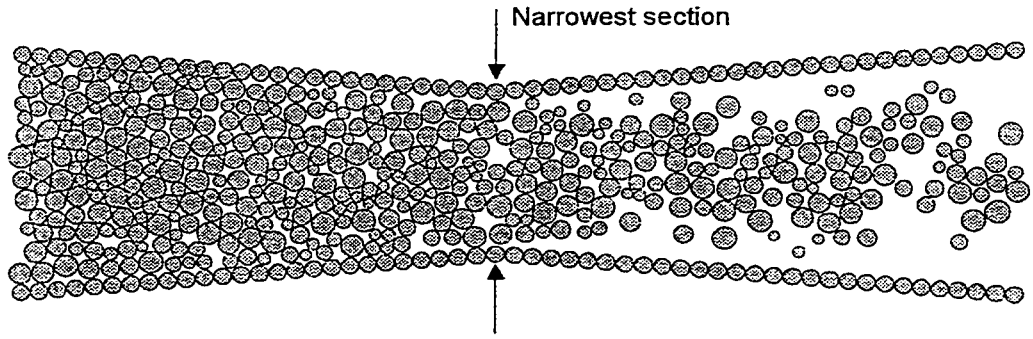

Figure 47: Ice transport in a channel with convergence (funnel shape).

The algorithm used in assessing the ice velocity and flux in a channel composed of various characteristic shapes can be separated into successive tasks presented in Figure 48.

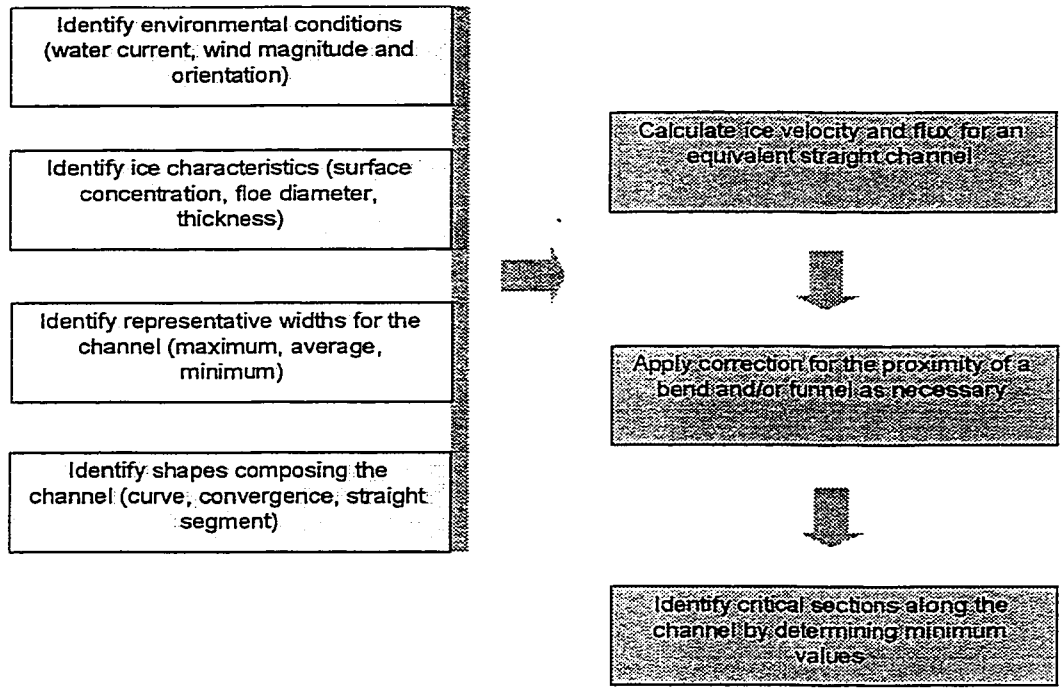

Figure 48: Algorithm for ice clearing calculation.

9.2 Integrated ice management

The Canadian Coast Guard is presently combining the relationships and algorithm developed in this study with other ice management components developed separately, such as an ice production model, in an integrated management system gets the benefits of the Pdyn model predictions, while avoiding the high cost of actually running the model. The parameters of the relationships developed from the Pdyn results and the suggested algorithm make use of data that is readily available to the Canadian Coast Guard through its monitoring program and, as such, can easily be integrated into the decision-support system. These inputs include:

Description of the general ambient conditions:

- wind magnitude and direction;
- water current;
- average ice concentration;
- ice representative floe size;
- average ice thickness;
- channel's hydraulic gradient;

Description of sections of interest:

- x- and y-coordinates of channel section;
- water depth;

The ice clearing module could provide the following outputs:

- Predicted ice flux and velocity at each of the sections of interest (from the relationships developed using the Pdyn model);
- Ackerman ice clearing capacity;
- Ratio of flow Froude number/critical Froude number to be used as an additional indicator of the potential for ice jam;

10 - CONCLUSIONS

Ice management is a complex task that involves the understanding of processes affecting ice formation and transport. These processes are typically difficult to quantify, measure, and predict, and although certain numerical models have been developed to simulate ice movement, their complexity and computational cost greatly limit their application for day-to-day management operations where timely results are needed.

The objective of the present study was to develop a simple, easy to use method of predicting the ice clearing capacity of a channel. The approach relied on the aggregation of a large number of model simulation results into relationships that would provide quantitative insight on the ice velocity and flux expected under various conditions. A large number of computer simulations were carried out using the Lagrangian particle-dynamics model Pdyn, under a wide range of conditions. The results not only showed the impacts of various factors, such as channel geometry and wind conditions, on the ice clearing capacity, but also lead to the development of two relationships (Equation 30) that relate these factors to the ice velocity and flux.

The relationships obtained incorporate the impact of a wide range of environmental factors (channel width, water current, ice concentration, ice

thickness, ice floe diameter, and wind), while being simple to apply in day-to-day operations because of their use of readily available data.

11 - BIBLIOGRAPHY

Ackerman, N. L., Shen, H. T. and Ruggles, R.W. (1981): *Transportation of Ice in Rivers*, in Proceedings of the IAHR Symposium on Ice, pp. 333-346.

Ackerman, N. L. and Shen, H. T. (1983): *Mechanics of Ice Formation in Rivers*, CRREL Report 83-31, 14 p.

Ashton, G.D. (1986): *River and Lake Ice Engineering*, Water Resources Publications, 485 pp.

Belthaos, S. (1983): *River Ice Jams: Theory, Case Studies and Applications*, Journal of Hydraulic Engineering, Vol. 109, No. 10, pp. 1338-1359.

Belthaos, S. (1995): *River Ice Jams*, Water Resources Publications, 372 pp.

Belthaos, S., Burrell, B., and Ismal, S. (1996): *1991 Ice Jamming Along the Saint-John River: A Case Study*, Canadian Journal of Civil Engineering, Vol. 23, No. 2, pp. 381-394.

Calkins, D.J., and Ashton, G.D. (1975): *Arching of Fragmented Ice Covers*, Canadian Journal of Civil Engineering, Vol. 2 (4), pp. 392-399.

Calkins, D.J., Hutton, M.S., and Marlar, T.L. (1976): *Analysis of Potential Ice Jam Sites on the Connecticut River at Windsor, Vermont*, CRREL Report 76-31, 31 p.

Canadian Committee on River Ice Processes and the Environment (1997): *Short Course on River Ice Science and Engineering*, Lecture Notes of the 9th Workshop on River ice, September 23-24, Fredericton, N.B. (Hydrology Section of the Canadian Geophysical Union).

Carlson, R.F., Zarling, J.P., and Link, L.E. (1989): *Cold Region Engineering Research - Strategic Plan*, Journal of Cold Regions Engineering, ASCE, Vol. 3, No. 4, pp. 172-190.

Crissman, R.D., Ettema, R., Andres, D. and Carson, R. (1995): *Ice Jamming in Upper Niagara River: Processes and Plan of Study*, in Journal of Cold Region Engineering, Vol. 9, No. 2, pp. 89-104.

Davar, K.S., Beltaos, S., and Pratte B. (1996): *A Primer on Hydraulics of Ice Covered Rivers*, Report of the Canadian Committee on River Ice Processes and the Environment, 191 p.

Dumont, S. (1997): *La gestion des glaces dans le tronçon Québec-Montréal du fleuve Saint-Laurent*, Bilan de la situation, Report, Canadian Coast Guard, Laurentian Region.

Environment Canada (1996): *State of the Environment Report on the St. Lawrence River, Volume 1: The St. Lawrence Ecosystem*, Environment Canada - Quebec Region, 600 pp.

Ettema, R. (1990): *Jam Initiation in Unobstructed Channels: Laboratory Observations*, Journal of Hydraulic Research, IAHR, 28(6), pp. 673-684.

Ettema, R., Muste, M., Kruger, A., and Zufelt, J. (1997): *Factors Influencing Ice Conveyance at River Confluences*, CRREL, Special Report 97-34, U.S. Army Corps of Engineers, December 1997.

Frankenstein, G.E., and Assur, A. (1972): *Israel River Ice Jam*, Proceedings of the IAHR Symposium on Ice and Its Action, Vol. 2, pp. 153-157.

Helsel, D.R., and Hirsh, R.M. (1992): *Statistical Methods in Water Resources*, Studies in Environmental Science 49, Elseview Science Publishing Company, 522 p.

IAHR Working Group on River Ice Hydraulics (1986): *River Ice Jams*: A stage of the Art Report.

Laboratoire Lasalle (1959): *Les problèmes de la glace dans les structures hydrauliques*, Proceedings of the 8th Conference of AIHR.

Lal, A.M.W., and Shen, H.T. (1991): *Mathematical Model for River Ice Processes*, Journal of Hydraulic Engineering, Vol. 117, No. 7, July, pp. 851-867.

Lawrie C.J.R. (1972): *Ice Control Measures on the St.Lawrence River*, Report, Transport Canada, 12 p.

Marcotte, N. (1975): *Heat Transfer from Open-Water Surfaces in Winter*, National Research Council, Technical Memorandum No. 114, pp. 2-16.

Michel, B. (1971): *Winter Regime of Rivers and Lakes*, CRREL, Cold Regions Science and Engineering Monograph III-B1a, 131p.

Morse, B. (1994): *Embâcles sur le lac St-Pierre*, Report, Canadian Coast Guard, Laurentian Region.

Nuttall, J.B. (1973): *River Modifications and Channel Improvements*, Seminar on Ice Jams in Canada, University of Alberta, NRC Technical Memo No. 107, pp. 83-91.

Sayed, M. (1997): *Discrete and Lattice Models of Floating Ice Covers*, Proceedings of the 7th International Offshore and Polar Engineering Conference, Honolulu, USA, pp. 428-433.

Sayed, M., and Carriere, T. (1999): *Overview of a new Operational Ice Model*,

Proceedings of ISOPE-99, Brest, France, May 30 – June 4, 1999.

Sayed, M., Neralla, V.R., and Savage S.B. (1995): *Yield Conditions of an Assembly of Discrete Ice Floes*, Proceedings of the 5th International Offshore and Polar Engineering Conference, La Hague, The Netherlands, pp. 330-335.

Sayed, M., Serrer, M., and Arden D.A. (1994): *Numerical Simulations of Ice Jams in Lake St.Peter*, Report IECE-CRT-CTR-004, National Research Council Canada, 29 p.

Serrer, M., Sayed M., Crookshank, N., and Zhang J. (1997): *Numerical Simulations of Ice Flow at Curve 2*, Lake St. Peter, Report HYD-TR-019, National Research Council Canada, 80 pp.

Shen, H.T., and Yappa, P.D. (1984): *Computer Simulation of Ice Cover Formation in the Upper St-Lawrence River*, Proceeding of the 3rd Workshop on Hydraulics of River Ice, Fredericton, Canada, pp. 227-245.

Shen, H.T., Chen, Y.C., Wake, A., and Crissman, R.D. (1993): *Lagrangian Discrete Parcel Simulation of River Ice Dynamics*, Proceedings of the 3rd International Offshore and Polar Engineering Conference, Singapore, June 1993, pp. 562-566.

Shen, H.T., Shen, H. and Tsai, S. (1990): *Dynamic Transport of River Ice*, in Journal of Hydraulic Research, Vol. 28, No.6, pp. 659-671.

Shen, H.T., Wang, D.S., and Lal, A.M.W. (1993): *A River Ice Simulation Model – RICEN: Model Formulation and Program Guide*, Report 93-7, Department of Civil and Environmental Engineering, Clarkson University, 109 p.

Shen, H.T., and Wang, D.S. (1995): *Under Cover Transport and Accumulation of Frazil Granules*, Journal of Hydraulic Engineering, Vol. 121, No. 2, pp. 184-194.

Shen, H.T., and Lu, S. (1996): *Dynamics of River Ice Jam Release*, Proceedings of the International Conference on Cold Region Engineering, ASCE, pp. 594-604.

Siles, J. (1997): *Rapport sur les activités de conception du programme de prédiction de volume de glace formée*, Report, Canadian Coast Guard, 37 p.

Tatinclaux, J-C., and Lee, C.L. (1978): *Initiation of Ice Jams – A Laboratory Study*, Canadian Journal of Civil Engineering, Vol. 5 (2), pp. 202-212.

Urroz, G.E., and Ettema, R. (1994): *Ice Accumulation Rate and the Geometry of Ice Jams in River Bends*, Proceedings of the National Conference on Hydraulic Engineering, ASCE, pp. 386-390.

Urroz, G.E. and Ettema, R. (1994): *Small-scale experiments on ice-jam initiation*

in a curved channel, Canadian Journal of Civil Engineering, No. 21, pp. 719-727.

Wang, D.S., Shen, H.T. and Crissman, R.D. (1995): *Simulation and Analysis of Upper Niagara River Ice-Jam Conditions*, Journal of Cold Region Engineering, Vol. 9 No. 3, pp.119-134.

White, K.D. (1994): *Ice Jam Data Collection*, CRREL Special Report 94-7, 37 p.

APPENDIX A: SUMMARY OF SIMULATIONS RESULTS

Table A.1: Simulations with straight channel, average ice velocity and flux at Section 2 (1.0-2.0 h)

ID	Channel Width (m)	Water Current (m/s)	Initial Ice Concent.	Ice Thickness (m)	Ice floe radius (m)	Wind direction	Wind magnitude (knots)	Ice velocity (m/s)	Ice flux (m^2/s)
1	180	0.30	0.81	0.50	12.50	0	0	0.28	37.2
2	180	0.50	0.81	0.50	12.50	0	0	0.48	56.3
3	180	0.70	0.81	0.50	12.50	0	0	0.68	75.7
4	180	0.85	0.81	0.50	12.50	0	0	0.73	78.7
5	180	1.00	0.81	0.50	12.50	0	0	0.88	102.8
6	180	0.50	0.70	0.50	12.50	0	0	0.49	54.1
7	180	0.50	0.60	0.50	12.50	0	0	0.50	52.6
8	180	0.50	0.55	0.50	12.50	0	0	0.50	50.2
9	210	0.30	0.80	0.50	12.50	0	0	0.30	44.5
10	210	0.50	0.80	0.50	12.50	0	0	0.48	66.6
11	210	0.70	0.80	0.50	12.50	0	0	0.69	94.3
12	210	0.85	0.80	0.50	12.50	0	0	0.84	114.8
13	210	1.00	0.80	0.50	12.50	0	0	0.99	132.8
14	210	0.30	0.55	0.50	12.50	0	0	0.30	35.6
15	210	0.30	0.70	0.50	12.50	0	0	0.30	44.2
16	210	0.30	0.75	0.50	12.50	0	0	0.30	46.4
17	210	0.30	0.80	0.35	12.50	0	0	0.28	42.5
18	210	0.30	0.80	0.75	12.50	0	0	0.30	44.5
19	210	0.30	0.80	1.00	12.50	0	0	0.30	46.6
20	240	0.15	0.83	0.50	12.50	0	0	0.15	26.2
21	240	0.30	0.83	0.50	12.50	0	0	0.29	51.1
22	240	0.50	0.83	0.50	12.50	0	0	0.50	81.6
23	240	0.70	0.83	0.50	12.50	0	0	0.65	103.4
24	240	0.85	0.83	0.50	12.50	0	0	0.84	138.0
25	240	1.00	0.83	0.50	12.50	0	0	0.99	154.3
26	240	1.15	0.83	0.50	12.50	0	0	1.14	171.8
27	240	1.30	0.83	0.50	12.50	0	0	1.26	184.6
28	240	0.30	0.66	0.50	12.50	0	0	0.30	46.3
29	240	0.30	0.70	0.50	12.50	0	0	0.30	50.2
30	240	0.30	0.74	0.50	12.50	0	0	0.30	49.3
31	240	0.30	0.83	0.35	12.50	0	0	0.29	49.9
32	240	0.30	0.83	0.75	12.50	0	0	0.30	53.1
33	240	0.30	0.83	1.00	12.50	0	0	0.30	53.5
34	240	0.50	0.83	0.35	12.50	0	0	0.48	77.6
35	240	0.50	0.83	0.75	12.50	0	0	0.50	86.6
36	240	0.50	0.83	1.00	12.50	0	0	0.50	87.4
37	240	0.70	0.83	0.35	12.50	0	0	0.67	108.1
38	240	0.70	0.83	0.75	12.50	0	0	0.70	118.6
39	240	0.70	0.83	1.00	12.50	0	0	0.70	119.5
40	240	0.30	0.80	0.50	15.00	0	0	0.29	51.2
41	240	0.50	0.80	0.50	15.00	0	0	0.50	84.5
42	240	0.70	0.80	0.50	15.00	0	0	0.68	109.7
43	240	0.30	0.82	0.50	10.00	0	0	0.30	50.7
44	240	0.50	0.82	0.50	10.00	0	0	0.48	75.9
45	240	0.70	0.82	0.50	10.00	0	0	0.65	105.6
46	270	0.30	0.81	0.50	12.50	0	0	0.29	59.0
47	270	0.50	0.81	0.50	12.50	0	0	0.49	95.0
48	270	0.70	0.81	0.50	12.50	0	0	0.70	128.6
49	270	0.85	0.81	0.50	12.50	0	0	0.83	149.5
50	270	1.00	0.81	0.50	12.50	0	0	0.98	175.4
51	300	0.30	0.83	0.50	12.50	0	0	0.30	65.5
52	300	0.50	0.83	0.50	12.50	0	0	0.50	105.2
53	300	0.70	0.83	0.50	12.50	0	0	0.70	152.6
54	300	0.85	0.83	0.50	12.50	0	0	0.84	181.9

ID	Channel Width (m)	Water Current (m/s)	Initial Ice Concent.	Ice Thickness (m)	Ice floe radius (m)	Wind direction	Wind magnitude (knots)	Ice velocity (m/s)	Ice flux (m^2/s)
55	300	1.00	0.83	0.50	12.50	0	0	0.99	192.3
56	210	0.30	0.80	0.50	12.50	45	5	0.20	31.5
57	210	0.30	0.80	0.50	12.50	45	10	0.12	19.6
58	210	0.30	0.80	0.50	12.50	45	15	0.06	10.3
59	210	0.30	0.80	0.50	12.50	45	20	0.00	0.8
60	210	0.30	0.80	0.50	12.50	0	10	0.14	21.7
61	210	0.30	0.80	0.50	12.50	0	20	0.00	-0.2
62	240	0.30	0.83	0.50	12.50	45	10	0.12	23.0
63	240	0.30	0.83	0.50	12.50	45	15	0.07	12.9
64	240	0.30	0.83	0.50	12.50	45	20	0.00	0.9
65	240	0.30	0.83	0.50	12.50	0	10	0.14	25.1
66	240	0.30	0.83	0.50	12.50	0	15	0.06	11.3
67	240	0.30	0.83	0.50	12.50	0	20	0.00	-0.4
68	240	0.30	0.82	0.50	12.50	180	10	0.44	75.5
69	240	0.30	0.82	0.50	12.50	225	10	0.32	58.0
70	240	0.30	0.82	0.50	12.50	22.5	10	0.12	21.7
71	240	0.30	0.82	0.50	12.50	90	10	0.21	37.3

Table A.2: Simulations with funnel channel, average ice velocity and flux at Section 3 (1.0-2.0 h)

ID	Convergence	Water Current (m/s)	Initial Ice Concent.	Ice Thickness (m)	Ice floe radius (m)	Wind direction	Wind magnitude (knots)	Ice velocity (m/s)	Ice flux (m^2/s)
1	Sharp	0.30	0.69	0.50	12.50	0	0	0.26	36.8
2	Sharp	0.70	0.69	0.50	12.50	0	0	0.50	70.3
3	Sharp	0.85	0.69	0.50	12.50	0	0	0.59	81.3
4	Sharp	1.00	0.69	0.50	12.50	0	0	0.68	92.8
5	Sharp	0.30	0.69	0.50	12.50	0	5	0.21	29.0
6	Sharp	0.30	0.69	0.50	12.50	0	10	0.04	6.0
7	Smooth	0.30	0.52	0.50	12.50	0	0	0.24	37.5
8	Smooth	0.50	0.52	0.50	12.50	0	0	0.37	57.3
9	Smooth	0.70	0.52	0.50	12.50	0	0	0.48	75.7
10	Smooth	0.85	0.52	0.50	12.50	0	0	0.55	86.0
11	Smooth	1.00	0.52	0.50	12.50	0	0	0.65	99.0

Table A.3: Simulations with curved channel, average ice velocity and flux at Section 3 (1.0-2.0 h)

ID	Curvature	Water Current (m/s)	Initial Ice Concent.	Ice Thickness (m)	Ice floe radius (m)	Wind direction	Wind magnitude (knots)	Ice velocity (m/s)	Ice flux (m^2/s)
1	Sharp	0.30	0.60	0.50	12.50	0	0	0.09	10.81
2	Sharp	0.50	0.60	0.50	12.50	0	0	0.19	22.21
3	Sharp	0.70	0.60	0.50	12.50	0	0	0.25	29.60
4	Sharp	0.85	0.60	0.50	12.50	0	0	0.31	36.98
5	Sharp	1.00	0.60	0.50	12.50	0	0	0.38	43.19
6	Smooth	0.30	0.78	0.50	12.50	0	0	0.17	27.31
7	Smooth	0.50	0.78	0.50	12.50	0	0	0.28	43.90
8	Smooth	0.70	0.78	0.50	12.50	0	0	0.44	67.16
9	Smooth	0.85	0.78	0.50	12.50	0	0	0.58	85.67
10	Smooth	1.00	0.78	0.50	12.50	0	0	0.68	104.09